Hindawi
Advances in Astronomy
Volume 2022, Article ID 5364541, 29 pages
https://doi.org/10.1155/2022/5364541

Research Article

Some Bianchi Type Viscous Holographic Dark Energy Cosmological Models in the Brans–Dicke Theory

M. Vijaya Santhi,[1] T. Chinnappalanaidu,[1] S. Srivani Madhu,[1] and Daba Meshesha Gusu [1,2]

[1]*Department of Applied Mathematics, Andhra University, Visakhapatnam 530003, India*
[2]*Department of Mathematics, Ambo University, Ambo, Ethiopia*

Correspondence should be addressed to Daba Meshesha Gusu; dabam7@gmail.com

Received 15 June 2022; Revised 19 September 2022; Accepted 30 September 2022; Published 2 November 2022

Academic Editor: M. Sharif

In this article, we analyze Bianchi type–II, VIII, and IX spatially homogeneous and anisotropic space-times in the background of the Brans–Dicke theory of gravity within the framework of viscous holographic dark energy. To solve the field equations, we have used the relation between the metric potentials as $R = S^n$ and the relation between the scalar field ϕ and the scale factor a as $\phi = a^m$. Also, we have discussed some of the dynamical parameters of the obtained models, such as the deceleration parameter (q), the jerk parameter (j), the EoS parameter (ω_{vhde}), the density parameter (Ω_{vhde}), Om-diagnostic, squared speed of sound (v_s^2), EoS plane $(\omega_{vhde} - \omega_{vhde}')$, and statefinder plane $(r - s)$ through graphical representation, which are significant in the discussion of cosmology. Furthermore, all the models obtained and graphically presented shown an expanding and accelerating Universe, which is in better agreement with the latest experimental data. The viscous holographic dark energy models are compatible with explaining the present cosmic accelerated expansion.

1. Introduction

In 1905, the theory of Special Relativity (SR) [1–3] was put forward by A. Einstein, which shown the genesis of absolute space and absolute time by surpassing the single 4D space-time, which had only an absolute meaning [4]. The perception that the gravitational field in a small neighborhood of space-time is incomprehensible from a proper acceleration in the frame of reference (principle of equivalence), has taken an upturn from Special Relativity (SR) to General Relativity (GR), where the gravitation has been adjoined to SR (holds true only in the absence of gravitation), which eventually gives a curved space-time, as the SR is generalized for the accelerating observers. As an outcome of Mach's limitation of absolute space, as Einstein had anticipated, the idea of general covariance (the absence of an advantaged frame of reference) develops [5] and by default obeys Mach's principle. Apparently, this was not the case, since various anti-Machian elements were discovered in GR.

Although GR is undeniably an appealing theory [6–10], it fails to offer the ultimate interpretation of gravity (a paradigm of a perfect theory), disregarding all the advantages. The theory has several conceptual issues, most of which are often overlooked, in addition to its much-discussed incompatibility with quantum mechanics. If in space, consistent with the same old epitome, where 95% of the overall constituent material continues to be missing, its miles an intimidating sign for us to doubt back to the very foundations of the theory. A significant perspective with a prominent context of alternative theories of gravitation develops from a critical study of Mach's principle, the equivalence principle, dark energy (DE) and dark matter (DM), and so on. Over the years, alternative theories of gravity have continued to draw considerable interest, leading to the discussion of numerous theories. These theories offered the first potentially feasible alternatives to the conventional general relativistic theory of gravity as proposed by Einstein. One of them is scalar-tensor theories of gravitation, where the dynamical DE component is introduced in the

right-hand side of the Einstein field equations, and the other is modified theories of gravitation, where the left-hand side of the Einstein field equations are modified. Scalar-tensor theories have emerged as some of the most well-established and well-studied alternatives to conservative gravity theories in the literature.

The Brans–Dicke theory (BDT) [11] is the most natural choice as the scalar-tensor generalization of GR, which can be considered as a pioneer in the study of scalar-tensor theories, and the inclusion of Mach's Principle led to the advent of this theory. This can be called the first-ever theory of gravity, where the metric tensor represents the dynamics of space-time and the scalar field describes the dynamics of gravity. The BDT also gives a fair description of the early era, as well as the present phases of cosmic evolution that gives a proper explanation for the Universe's accelerated expansion [12], as this theory justifies the experiments in the Solar System domain [13]. The gravitational constant G in this theory is to be replaced with $1/\phi$, where ϕ purely depends on the time and is coupled to gravity with a coupling parameter ω. It is evident in the literature that GR can be retrieved from the BDT if ϕ is a constant and $\omega \longrightarrow \infty$ [14, 15]. As and when the coupling constant ω takes huge values greater than 500, GR can be deduced from BDT [16], accounting for the recent Universe's expansion and accommodating the observational data as well [17–19]. There is a prominent position for BDT among theories of gravitation because it is capable of accounting for the properties of cosmic expansion since the early phases of inflation [20]. A generalized (or modified) version of BDT [21–23] supports the notion that the parameter ω depends on the scalar field ϕ. Several models, based on the BDT, have been perfectly able to explain the properties of the expanding Universe with the help of various cosmological parameters [24–27]. The models based on the generalized BDT have an extremely low value for the coupling parameter, unaccommodating the findings during the implementation of the previous versions of the theory [20, 28–30]. A recent study in the BDT [31] has been made in the FRW models with a varying Λ-term and a dynamic deceleration parameter. Also, it has been recently justified that for huge values of ω, the generalization of BDT can explain the Universe's accelerated expansion with the interaction between matter and a scalar field [32].

The anisotropy and the spatial homogeneity are the two major characterizations for the Bianchi type (BT) cosmological models. There are nine different models altogether, and these have been classified into two classes [33]. The class-A represents the BT models I, II, VII, VIII, and IX, and class-B consists of BT models III, IV, V, VI, and VII. These models are known to describe the evolution of the Universe's early stages in the presence of various physical distributions of matter, thereby explaining the structure and space properties of all the Einstein field conditions along with cosmological arrangements, and thus, rewriting the Einstein equations in the Hamiltonian form. In this regard, Misner [34, 35] and other authors have focused much of their efforts on fabricating a fine Hamiltonian system. In spite of this, these Hamiltonian forms could not be utilized to prove the collapse speculations by Lin and Wald [36, 37]. These BT models uncover the magnitude of anisotropy in the background radiation and provide a pragmatic picture of the past eras in the history of the cosmos. Furthermore, the cosmological problem of Einstein field equations from a theoretical perspective can be addressed well through the anisotropic models, as they tend to have greater generality when compared with isotropic solutions. In particular, we are involved in studying the BT-II, VIII, and IX cosmological models in the presence of viscous holographic dark energy (VHDE) in BDT. Diverse aspects of the BT-II, VIII, and IX cosmological models have been explored by many authors [38–41].

Present-time experimental and theoretical supernovae type Ia (SNeIa) observations [42, 43], cosmic microwave background radiation (CMBR) [44, 45], and large-scale structures [45, 46] provide the most enthralling evidence for the same. Many models of the Universe have been studied assuming the existence of a mysterious component, so-called DE, which generates huge negative pressure, imparting the mechanism for the accelerated cosmic expansion. Planck's current measurements indicate that 68.3% of the Universe's total energy content is in the form of DE. In spite of the success of standard cosmology, it is known that there are a few unsolvable problems that include the search for accommodating DE candidates, in which researches found the cosmological constant as a primary candidate for DE that not only describes the phenomenon of DE but also the ``fine tuning" and "cosmic coincidence". For this reason, various dynamical DE models, which include a family of scalar fields such as quintessence [47–50], phantom [51–54], quintom [55, 56], tachyon [57–59], K-essence [60], and various Chaplygin gas models like generalized Chaplygin gas, extended Chaplygin gas, and modified Chaplygin gas [61–75], have been developed.

Way back then, viscosity played an influential role in the study of cosmology, which has been extended in recent years to include the study of an accelerating Universe and has acquired an immense interest in present times for numerous reasons. The idea of perfect fluid in the study of cosmic models has shown no dissipation and helps in the study of cosmic evolution. In the existent scenario, the study of imperfect fluid models has been suggested by introducing the concept of viscosity. In particular, the bulk viscous fluids that are included in the discourse of inflation are competent for explaining late-time cosmic acceleration. The increase in the viscosity is attributed to a Universe that is expanding at a rapid rate and can be understood as an accumulation of states that are out of thermal equilibrium in a small fraction of time. For these obvious reasons, the concept of viscosity has gained popularity in the study of space.

The holographic dark energy (HDE) models have seen success in recent years, with many considering them as the appropriate candidates to explain the problems of modern cosmology. The concept of HDE was initially introduced by Li [76] in 2004 with respect to the holographic principle [77–83] to elucidate the late-time Universe's accelerated expansion. The holographic principle, as stated by black hole thermodynamics [84, 85], says that a hologram can be completely represented as a volume of space, which agrees

with a theory related to the boundary of that space [86] and the AdS/CFT (anti-de Sitter/Conformal field theory) correspondence, as it can be observed in the seminal reference [87]. In [76], a holographic principle-based cosmic acceleration model was developed for the first time. As such, the reduced Plank mass and a cosmological length scale, taken as the future event horizon of the Universe, are the two physical quantities of the boundary of the Universe on which a DE model relies on. As a consequence of an ultraviolet cutoff (Λ) for a region of size L, where the mass of a black hole of the similar size is not exceeded by the total energy, HDE density can be stated as $\rho_\Lambda = 3C^2M_{Pl}/L^2$, with C being a constant, $M_{Pl} = 1/\sqrt{8\pi G}$ being the reduced Planck mass, and G being the Newtonian gravitational constant. The holographic principle is considered as a central principle of quantum gravity because of its applications in various fields of physics, viz. cosmology [88] and nuclear physics [89] in the present era. All the generalized HDE models known as of now are the suggested ones by [90], which came only after Li. Moreover, the Nojiri–Odintsov HDE gives a detailed description of covariant theories different from Li's HDE [91]. A more dynamical scenario for HDE in the BDT along with matter creation has been suggested instead of Einstein gravity because of the fact that a dynamical frame is necessary to accommodate the HDE density that belongs to a dynamical cosmological constant. Considering various IR cut-offs in the framework of the BDT, a number of authors [92–99] have explained the rapid expansion of the cosmos and have shown a solution to alleviate the cosmic coincidence problem. With the help of cosmic observational data, Xu et al. [100] have constructed the HDE model in BDT.

Motivated by the above discussions and investigations in the Bianchi space-times, we investigate the anisotropic BT–II, VIII, and IX space-times in the presence of VHDE. This paper is planned as, in Section 2, we explain the metric and field equations. In Section 3, we obtain the solutions of the field equations, along with some important properties of the Universe in Section 4. Lastly, the interpretations of our models are presented in the last section.

2. Metric and Field Equations

The spatially homogeneous BT metrics II, VIII, and IX of the form,

$$ds^2 = dt^2 - R^2\left[d\theta^2 + f^2(\theta)d\varphi^2\right] - S^2\left[d\psi + h(\theta)d\varphi\right]^2, \quad (1)$$

have been considered, where the Eulerian angles are represented as (θ, φ, ψ), R and S are a function of t only. It represents the following:

BT II if $f(\theta) = 1$ and $h(\theta) = \theta$;

BT VIII if $f(\theta) = \cosh\theta$ and $h(\theta) = \sinh\theta$;

BT IX if $f(\theta) = \sin\theta$ and $h(\theta) = \cos\theta$.

The action of BDT in the presence of matter with Lagrangian L_m in the canonical form (Jordan frame) is given by

$$S = \int d^4x\sqrt{-g}\left(-\phi\mathcal{R} + \frac{\omega}{\phi}\Box_\mu\phi\Box_\mu\phi + L_m\right), \quad (2)$$

where ϕ is the Brans–Dicke scalar field representing the inverse of Newton's constant, which is allowed to vary with space and time, $\mathcal{R}$ is the scalar curvature, and ω is the Brans–Dicke constant. Varying the action in (2) with respect to the metric tensor g_{ij} and the scalar field ϕ, the field equations are obtained as

$$G_{ij} = -8\pi\phi^{-1}T_{ij} - \omega\phi^{-2}\left(\phi_{,i}\phi_{,j} - \frac{1}{2}g_{ij}\phi_{,\kappa}\phi^{,\kappa}\right) - \phi^{-1}\left(\phi_{i;j} - g_{ij}\phi^{,\kappa}_{;\kappa}\right), \quad (3)$$

$$\phi^{,\kappa}_{;\kappa} = 8\pi(3 + 2\omega)^{-1}T, \quad (4)$$

where $G_{ij} = \mathcal{R}_{ij} - 1/2\mathcal{R}g_{ij}$ is an Einstein tensor, T_{ij} is the stress-energy tensor of the matter, and $\mathcal{R}_{ij}$ is the Ricci curvature tensor.

The conservation equation

$$T^{ij}_{;j} = 0, \quad (5)$$

is a consequence of the field equations (3) and (4).

The energy momentum tensor for the VHDE is taken as

$$T_{ij} = T^m_{ij} + T^h_{ij}. \quad (6)$$

Here, T^m_{ij} and T^h_{ij} represent matter and VHDE tensors, which are given as

$$T^h_{ij} = \left(\overline{P}_{vhde} + \rho_{vhde}\right)U^h_iU^h_j - \overline{P}_{vhde}g_{ij}, \quad T^m_{ij} = \rho_mU^m_iU^m_j, \quad (7)$$

where ρ_m is the energy density of the matter, $\overline{P}_{vhde}$ and ρ_{vhde}, respectively, represent the pressure and energy density of the VHDE; U_i denotes the comoving velocity vector of the matter and VHDE, satisfying $U_iU^i = 1$. The VHDE pressure satisfies the relation $\overline{P}_{vhde} = P_{vhde} - 3\zeta H$, where ζ is the bulk viscosity coefficient. Equation of state parameters for VHDE and HDE, respectively, are defined as $\omega_{vhde} = P_{vhde}/\rho_{vhde}$ and $\omega_{hde} = P_{hde}/\rho_{hde}$. The unification of viscosity and HDE is a mathematical attempt in the light of the holographic principle. Moreover, it is hypothesized that DE is pervading the whole Universe, with bulk viscosity giving the accelerated expansion of phantom types in the late time evolution of the Universe. Here, we have assumed pressure less DM and that the effective pressure of VHDE is a sum of the pressure of HDE and bulk viscosity. Eckart [101] has proposed a type of effective pressure in the context of general relativity. Recently, Singh and Srivastava [102] have considered VHDE for FRW space-time.

Now, with the help of equation (6), the field equations (3) and (4) for the metric in equation (1) can be written as

$$\frac{\ddot{R}}{R}+\frac{\ddot{S}}{S}+\frac{\dot{R}\dot{S}}{RS}+\frac{S^2}{4R^4}+\frac{\omega\dot{\phi}^2}{2\phi^2}+\frac{\dot{\phi}}{\phi}\left(\frac{\dot{R}}{R}+\frac{\dot{S}}{S}\right)+\frac{\ddot{\phi}}{\phi}=\frac{-8\pi\left(P_{vhde}-3\zeta H\right)}{\phi}, \tag{8}$$

$$\frac{2\ddot{R}}{R}+\frac{\dot{R}^2}{R^2}+\frac{\delta}{R^2}-\frac{3S^2}{4R^4}+\frac{\omega\dot{\phi}^2}{2\phi^2}+\frac{2\dot{R}\dot{\phi}}{R\phi}+\frac{\ddot{\phi}}{\phi}=\frac{-8\pi\left(P_{vhde}-3\zeta H\right)}{\phi}, \tag{9}$$

$$\frac{\dot{R}^2}{R^2}+\frac{\delta}{R^2}+\frac{2\dot{R}\dot{S}}{RS}-\frac{S^2}{4R^4}-\frac{\omega\dot{\phi}^2}{2\phi^2}+\frac{\dot{\phi}}{\phi}\left(\frac{2\dot{R}}{R}+\frac{\dot{S}}{S}\right)=\frac{8\pi\left(\rho_m+\rho_{vhde}\right)}{\phi}, \tag{10}$$

$$\&\quad \left(\frac{\dot{S}}{S}+\frac{2\dot{R}}{R}\right)\dot{\phi}+\ddot{\phi}=\frac{8\pi\left(\rho_m+\rho_{vhde}-3\left(P_{vhde}-3\zeta\right)H\right.}{3+2\omega}, \tag{11}$$

and the energy conservation equation becomes

$$\dot{\rho}_m+\dot{\rho}_{vhde}+\left(\frac{\dot{S}}{S}+\frac{2\dot{R}}{R}\right)\left(\rho_m+\rho_{vhde}+P_{vhde}-3\zeta H\right)=0. \tag{12}$$

Here, the over-head "dot" denotes differentiation with respect to 't'. When $\delta=0,\ -1,\ \&\ +1$, the field equations (8)–(11) correspond to the BT-II, VIII, and IX Universes, respectively. Now, by using the transformation $dt=R^2SdT$, the field equations (8)–(11) can be written as

$$\frac{R^{'}{}'}{R}+\frac{S^{'}{}'}{S}-\frac{2R^{'2}}{R^2}-\frac{S^{'2}}{S^2}-\frac{2R'S'}{RS}+\frac{S^4}{4}+\frac{\omega\phi^{'2}}{2\phi^2}+\frac{\phi^{'}{}'}{\phi}-\frac{R'\phi'}{R\phi}=\frac{-8\pi\left(P_{vhde}-3\zeta H\right)R^4S^2}{\phi}, \tag{13}$$

$$\frac{2R^{'}{}'}{R}-\frac{2R'S'}{RS}-\frac{3R^{'2}}{R^2}+\delta R^2S^2-\frac{3S^4}{4}+\frac{\omega\phi^{'2}}{2\phi^2}-\frac{\phi'S'}{\phi S}+\frac{\phi^{'}{}'}{\phi}=\frac{-8\pi\left(P_{vhde}-3\zeta H\right)R^4S^2}{\phi}, \tag{14}$$

$$\frac{R^2}{R^2}+\delta R^2S^2+\frac{2R'S'}{RS}-\frac{S^4}{4}-\frac{\omega\phi^{'2}}{2\phi^2}+\frac{\phi'}{\phi}\left(\frac{S'}{S}+\frac{2R'}{R}\right)=\frac{8\pi\left(\rho_m+\rho_{vhde}\right)R^4S^2}{\phi}, \tag{15}$$

$$\frac{\phi''}{R^4S^2}=\frac{8\pi\left(\rho_m+\rho_{vhde}-3\left(P_{vhde}-3\zeta H\right)\right)}{\phi}. \tag{16}$$

Also, the energy conservation equation leads to

$$\rho_m'+\rho_{vhde}'+\left(\frac{S'}{S}+\frac{2R'}{R}\right)\left(\rho_m+\rho_{vhde}+P_{vhde}-3\zeta H\right)=0. \tag{17}$$

The conservation equation of the matter is

$$\rho_m'+\left(\frac{S'}{S}+\frac{2R'}{R}\right)\rho_m=0, \tag{18}$$

and for VHDE, the conservation equation is

$$\rho_{vhde}'+\left(\frac{S'}{S}+\frac{2R'}{R}\right)\left(\rho_{vhde}+P_{vhde}-3\zeta H\right)=0. \tag{19}$$

Here, the over-head dash denotes differentiation with respect to "T."

3. Solutions of the Field Equations

Now, the set of equations (13)–(16) forms a system of four independent equations with seven unknowns: R, S, ϕ, ρ_m, ρ_{vhde}, P_{vhde}, and ζ. Hence, to find a determinate solution to these highly nonlinear differential equations, we need at least three physically viable conditions:

We assume that the relation between the metric potentials (Collins et al., [103]) as

$$R=S^n, \tag{20}$$

where $n>1$.

We consider the relation between scale factor a and scalar field ϕ (Tripathy et al., [104]) as

$$\phi=a^m, \tag{21}$$

where m is a positive constant.

We take the bulk viscosity coefficient in the following form (Ren and Meng [105]; Meng et al., [106])

$$\zeta=\zeta_0+\zeta_1H, \tag{22}$$

where ζ_0 and ζ_1 are positive constants and H is the Hubble parameter.

Now, using conditions (20) and (21) in field equations (13) and (14), we get

$$\frac{S''}{S}+\left(\frac{m(2n+1)-3}{3}\right)\frac{S'^2}{S^2}=\frac{\delta S^{2n+2}-S^4}{1-n}. \tag{23}$$

3.1. Bianchi Type- II ($\delta = 0$) Cosmological Model. If $\delta = 0$, equation (23) can be written as

$$\frac{S''}{S}+\left(\frac{m(2n+1)-3}{3}\right)\frac{S'^2}{S^2}=\frac{-S^4}{1-n}. \tag{24}$$

On solving equation (24), we get

$$\begin{aligned} S&=\left[2\beta_1-2\gamma_1 T\right]^{-1/2},\\ R&=\left[2\beta_1-2\gamma_1 T\right]^{-n/2}. \end{aligned} \tag{25}$$

where, $\gamma_1 = (2/(n-1)(6+2k_1))^{1/2}$, with $k_1 = m(2n+1) - 3/3$, whereas β_1 is an integration constant and $n > 1$.

The spatial volume and average scale factor are given by

$$V = R^2 S f(\theta) = \left(2\beta_1 - 2T\gamma_1\right)^{-2n-1/2}, \tag{26}$$

$$a = \left(R^2 S f(\theta)\right)^{1/3} = \left(2\beta_1 - 2T\gamma_1\right)^{-2n-1/6}. \tag{27}$$

From equations (27) and (21), the scalar field ϕ is given by

$$\phi = \left[2\beta_1 - 2\gamma_1 T\right]^{-m(2n+1)/6}. \tag{28}$$

The pressure of the VHDE is

$$P_{vhde} = \frac{\Upsilon_1}{576\pi\left(T\gamma_1 - \beta_1\right)^2}, \tag{29}$$

where

$$\begin{aligned} \Upsilon_1 =& \left((64\left(3+\left(n+\frac{1}{2}\right)m\right)\left(T\gamma_1-\beta_1\right)^3\gamma_1^2\left(n+\frac{1}{2}\right)m\left(2\beta_1-2T\gamma_1\right)^{(-2n-1)m+12n-12/6}\right.\\ &-144n^2\gamma_1^2\left(T\gamma_1-\beta_1\right)^2\left(2\beta_1-2T\gamma_1\right)^{(-2n-1)m+12n-6/6}\\ &+8\left(T\gamma_1-\beta_1\right)\left(\frac{-27}{8}+\left(\left(n+\frac{1}{2}\right)^2\omega m^2+\left(-3n-\frac{3}{2}\right)m-\frac{27n^2}{2}+9n\right)\gamma_1^2\right)\left(2\beta_1-2T\gamma_1\right)^{(-2n-1)m+12n/6}\\ &\left.-576\left(\left(T\zeta_0-\frac{\zeta_1 n}{3}-\frac{\zeta_1}{6}\right)\gamma_1-\beta_1\zeta_0\right)\pi\gamma_1\left(n+\frac{1}{2}\right)\right)\Bigg\}, \end{aligned} \tag{30}$$

The energy density of the matter is

$$\rho_m = \beta_2\left(2\beta_1 - 2\gamma_1 T\right)^{2n+1/2}, \tag{31}$$

where β_2 is the constant of integration.

The energy density of the VHDE is

$$\rho_{vhde} = \frac{\Upsilon_2}{576\pi\left(T\gamma_1 - \beta_1\right)}, \tag{32}$$

where

$$\Upsilon_2 = \left(\left(9+\left(8\omega\left(n+\frac{1}{2}\right)^2m^2-48\left(n+\frac{1}{2}\right)^2m-36n^2-72n\right)\gamma_1^2\right)\left(2\beta_1-2T\gamma_1\right)^{(-2n-1)m+12n/6}-576\pi\beta_2\left(2\beta_1-2T\gamma_1\right)^{n+1/2}\left(T\gamma_1-\beta_1\right)\right)\Bigg\}\Bigg\}. \tag{33}$$

The viscosity coefficient is given by

$$\zeta = \zeta_0 + \frac{\zeta_1\gamma_1(2n+1)}{3\left(2\beta_1 - 2\gamma_1 T\right)}. \tag{34}$$

Now the metric (1) can be written as

$$\begin{aligned} ds^2 =& dt^2 - \left[2\beta_1 - 2\gamma_1\right]^{-n}\left[d\theta^2 + d\varphi^2\right]\\ &-\left[2\beta_1 - 2\gamma_1\right]^{-1}\left[d\psi + \theta d\varphi\right]^2. \end{aligned} \tag{35}$$

3.2. Bianchi Type-VIII ($\delta = -1$) Cosmological Model. If $\delta = -1$, equation (23) can be written as

$$\frac{S''}{S}+\left(\frac{m(2n+1)-3}{3}\right)\frac{S'^2}{S^2}=\frac{-S^{2n+2}-S^4}{1-n}. \tag{36}$$

We can solve the above equation and get the deterministic solution only for $n = -1$.

Thus, from the equation (36), we get

$$S'^2 = \beta_3^2 S^6 + \gamma_2^2 S^2, \tag{37}$$

where $\beta_3^2 = 1/2k_2 - 6$ and $\gamma_2^2 = 1/2k_2 - 2$ with $k_2 = m + 3/3$.

From the equation (37), we get

$$S = \left[\frac{\gamma_2}{\beta_3}\operatorname{cosech}\left(2\gamma_2 T\right)\right]^{1/2},$$
$$R = \left[\frac{\gamma_2}{\beta_3}\operatorname{cosech}\left(2\gamma_2 T\right)\right]^{-1/2}. \tag{38}$$

The spatial volume and an average scale factor are given by

$$V = \cosh\theta\left[\frac{\gamma_2}{\beta_3}\operatorname{cosech}\left(2\gamma_2 T\right)\right]^{-1/2}, \tag{39}$$

$$a = (\cosh\theta)^{\frac{1}{3}}\left[\frac{\gamma_2}{\beta_3}\operatorname{cosech}\left(2\gamma_2 T\right)\right]^{-1/6}. \tag{40}$$

From equations (40) and (21), the scalar field ϕ is given by

$$\phi = \left[\frac{\gamma_2}{\beta_3}\operatorname{cosech}\left(2\gamma_2 T\right)\right]^{-m/6}(\cosh\theta)^{m/3}. \tag{41}$$

The pressure of the VHDE is

$$P_{vhde} = \frac{\Upsilon_3}{-144\pi\beta_3^3\sinh^3\left(2\gamma_2 T\right)}, \tag{42}$$

where

$$\Upsilon_3 = \left(\left(\cosh^{\frac{m}{3}}(\theta)\left(\frac{\gamma_2}{\beta_3}\operatorname{cosech}\left(2\gamma_2 T\right)\right)^{\frac{-m}{6}}\left(\left(-18+\left(18+(\omega+2)m^2+6m\right)\gamma_2^2\right)\beta_3^2\cosh^2\left(2\gamma_2 T\right)+\left(18+(-12m-72)\gamma_2^2\right)\beta_3^2-\frac{27\gamma_2^2}{2}\right),\right.$$
$$\left.-144\beta_3^3\left(\cosh\left(2\gamma_2 T\right)\sinh\left(2\gamma_2 T\right)\frac{\zeta_1\gamma_2}{3}+\cosh^2\left(2\gamma_2 T\right)\zeta_0-\zeta_0\right)\cosh\left(2\gamma_2 T\right)\pi\right)\gamma_2\right)\Bigg\}. \tag{43}$$

The energy density of the matter has the following expression:

$$\rho_m = \beta_4\left[\frac{\gamma_2}{\beta_3}\operatorname{cosech}\left(2\gamma_2 T\right)\right]^{1/2}, \tag{44}$$

where β_4 is an integration constant.

The energy density of the VHDE is obtained as

$$\rho_{vhde} = \frac{\Upsilon_4}{288\pi\beta_3^3\sinh^3\left(2\gamma_2 T\right)}, \tag{45}$$

where

$$\Upsilon_4 = \left(-2\gamma_2\cosh^{m/3}(\theta)\left(\left(18+\left(m^2\omega-6m+18\right)\gamma_2^2\right)\beta_3^2\cosh^2\left(2\gamma_2 T\right)-18\beta_3^2+\frac{9\gamma_2^2}{2}\right)\left(\frac{\gamma_2}{\beta_3}\operatorname{cosech}\left(2\gamma_2 T\right)\right)^{-m/6},\right.$$
$$\left.-288\beta_4\left(\frac{\gamma_2}{\beta_3}\operatorname{cosech}\left(2\gamma_2 T\right)\right)^{1/2}\sinh\left(2\gamma_2 T\right)\pi\beta_3^3\left(\cosh^2\left(2\gamma_2 T\right)-1\right)\right)\Bigg\}. \tag{46}$$

The viscosity coefficient is given by

$$\zeta = \zeta_0 + \frac{\zeta_1\gamma_2\coth\left(2\gamma_2 T\right)}{3}. \tag{47}$$

Hence, the metric (1) takes the following form:

$$ds^2 = dt^2 - \left[\frac{\gamma_2}{\beta_3}\operatorname{cosech}\left(2\gamma_2 T\right)\right]^{-1}\left[d\theta^2+\cosh\theta d\varphi^2\right]-\left[\frac{\gamma_2}{\beta_3}\operatorname{cosech}\left(2\gamma_2 T\right)\right][d\psi+\sinh\theta d\varphi]^2. \tag{48}$$

3.3. Bianchi Type-IX ($\delta = 1$) Cosmological Model. If $\delta = 1$, equation (23) can be written as

$$\frac{S''}{S} + \left(\frac{m(2n+1)-3}{3}\right)\frac{S'^2}{S^2} = \frac{S^{2n+2} - S^4}{1-n}. \tag{49}$$

We can solve the above equation and get the deterministic solution only for $n = -1$.

So, from equation (49), we get

$$S'^2 = \gamma_3^2 S^2 - \beta_5^2 S^6, \tag{50}$$

where, $\beta_5^2 = 1/6 - 2k_3$ and $\gamma_3^2 = 1/2 - 2k_3$ with $k_3 = m + 3/3$.

From equation (49), we get

$$S = \left[\frac{\gamma_3}{\beta_5}\operatorname{sech}(2\gamma_3 T)\right]^{1/2}, \qquad R = \left[\frac{\gamma_3}{\beta_5}\operatorname{sech}(2\gamma_3 T)\right]^{-1/2}. \tag{51}$$

The spatial volume and average scale factor are given by

$$V = \sin\theta\left[\frac{\gamma_3}{\beta_5}\operatorname{sech}(2\gamma_3 T)\right]^{-1/2}, \tag{52}$$

$$a = (\sin\theta)^{1/3}\left[\frac{\gamma_3}{\beta_5}\operatorname{sech}(2\gamma_3 T)\right]^{-1/6}. \tag{53}$$

From equations (21) and (53), the scalar field ϕ is given by

$$\phi = \left[\frac{\gamma_3}{\beta_5}\operatorname{sech}(2\gamma_3 T)\right]^{-m/6}(\sin\theta)^{m/3}. \tag{54}$$

The pressure of the VHDE is as follows:

$$P_{vhde} = \frac{\Upsilon_5}{-144\pi\beta_5^3\cosh^3(2\gamma_3 T)}, \tag{55}$$

where

$$\Upsilon_5 = \left(\left(\left(\left(-18 + \left(18 + (\omega+2)m^2 + 6m\right)\gamma_3^2\right)\beta_5^2\cosh^2(2\gamma_3 T) - \gamma_3^2\left(\frac{27}{2} + \left(-54 + (\omega+2)m^2 - 6m\right)\beta_5^2\right)\gamma_3^2\right)\sin^{m/3}(\theta)\left(\frac{\gamma_3}{\beta_5}\operatorname{sech}(2\gamma_3 T)\right)^{-m/6}\right.\right.$$
$$\left.\left. - 48\cosh(2\gamma_3 T)\pi\beta_5^3\left(\cosh^2(2\gamma_3 T)\zeta_1\gamma_3 + 3\sinh(2\gamma_3 T)\zeta_0\cosh(2\gamma_3 T) - \zeta_1\gamma_3\right)\right)\gamma_3\right). \tag{56}$$

The energy density of the matter is obtained as

$$\rho_m = \beta_6\left[\frac{\gamma_3}{\beta_5}\operatorname{sech}(2\gamma_3 T)\right]^{1/2}, \tag{57}$$

the energy density of the VHDE has the following expression:

$$\rho_{vhde} = \frac{\Upsilon_6}{288\pi\beta_5^3\cosh^3(2\gamma_3 T)}, \tag{58}$$

where

$$\Upsilon_6 = \left(-2\sin^{m/3}(\theta)\gamma_3\left(\left(-18 + \left(\left(m^2\omega - 6m + 18\right)\gamma_3^2\right)\beta_5^2 t\cosh^2 n(2\gamma_3 T)q - h\gamma_3^2\left(\frac{-9}{2} + \left(m^2\omega - 6m + 18\right)\beta_5^2\right)\gamma_3\left(\frac{\gamma_3}{\beta_5}\operatorname{sech}(2\gamma_3 T)\right)^{-m/6}\right.\right.\right.$$
$$\left.\left.\left. - 288\beta_6\left[\frac{\gamma_3}{\beta_5}\operatorname{sech}(2\gamma_3 T)\right]^{1/2}\pi\beta_5^3\cosh^3(2\gamma_3 T)\right)\right). \tag{59}$$

The viscosity coefficient is

$$\zeta = \zeta_0 + \frac{\zeta_1\gamma_3\tanh(2\gamma_3 T)}{3}. \tag{60}$$

Hence, the metric (1) can be written as

$$ds^2 = dt^2 - \left[\frac{\gamma_3}{\beta_5}\operatorname{sech}(2\gamma_3 T)\right]^{-1}\left[d\theta^2 + \sin\theta d\varphi^2\right] - \left[\frac{\gamma_3}{\beta_5}\operatorname{sech}(2\gamma_3 T)\right][d\psi + \cos\theta d\varphi]^2. \tag{61}$$

Thus, equations (35), (48), and (61) represent spatially homogeneous and anisotropic BT-II, VIII, and IX VHDE cosmological models, respectively, in the Brans–Dicke scalar theory of gravitation. For graphical representation we consider the following vales: $n = 1.9$, $m = 0.97$ for BT-II, $m = 0.011$ for BT-VIII, $m = 3.999$ for BT-IX, $\gamma_1 = -0.099$,

$\beta_1 = 0.145$, $\beta_2 = -1045$, $\omega = 958899$, $\zeta_1 = 9.15, 018.3$, $\zeta_0 = 0.35, 02$, $\gamma_2 = 0.099$, $\beta_3 = 0.045$, $\beta_4 = -9995$, $\gamma_3 = 0.095$, $\beta_5 = 0.011$, $\beta_6 = -999$, $a_0 = 1.5$, $H_0 = 85$. The plots of VHDE pressure (P_{vhde}) against redshift respectively for BT-II, VIII, and IX models have been represented in Figures 1–3for different values of ζ_0 & ζ_1. Here, we observe that the behavior of P_{vhde} for three different values of ζ_0 & ζ_1 is the increasing with redshift and varies in the negative region, which indicates the cosmic expansion. Moreover, as increasing the values of ζ_0 & ζ_1, we get more acceleration of the Universe. Also, we have depicted the energy density of VHDE (ρ_{vhde}) versus redshift in Figures 4–6 for BT–II, VIII. and IX models, respectively, and we observe that the trajectory varies in the positive region, which indicates an accelerated expansion of the cosmos. The bulk viscous coefficient has been plotted against redshift with various values of ζ_0 and ζ_1 in Figures 7–9 for BT-II, VIII, and IX models, respectively. The trajectories vary in positive regions throughout the evolution of all the three models for various values of ζ_0 and ζ_1, which indicates an accelerated expansion of the Universe.

Some of the cosmological properties of the models are discussed as follows:

The mean Hubble parameter H is given by

$$H = \frac{H_1 + H_2 + H_3}{3}, \tag{62}$$

where $H_1 = H_2 = \dot{R}/R, H_3 = \dot{S}/S$ are directional Hubble's parameters, which express the expansion rates of the Universe in the directions of x, y, and z, respectively. The mean Hubble's parameter of BT-II, VIII, and IX VHDE cosmological models are, respectively, given by

$$\begin{aligned} H &= \frac{\gamma_1 (2n+1)}{3(2\beta_1 - 2\gamma_1 T)}, \\ H &= \frac{\gamma_2 \coth(2\gamma_2 T)}{3}, \\ H &= \frac{\gamma_3 \tanh(2\gamma_3 T)}{3}. \end{aligned} \tag{63}$$

The anisotropic parameter of the BT-II VHDE model is given by

$$A_h = \frac{1}{3}\sum_{i=1}^{3}\left(\frac{H_i - H}{H}\right)^2 = \frac{2(n-1)^2}{(2n+1)^2}, \tag{64}$$

and for the BT-VIII and IX VHDE cosmological models, we get

$$A_h = 8. \tag{65}$$

From equations (64) and (65), we can observe that $A_h \neq 0$, which indicates that the BT-II, VIII, and IX models are always anisotropic throughout the evolution of the Universe with respect to VHDE.

The expansion scalar (ϑ) has been defined as

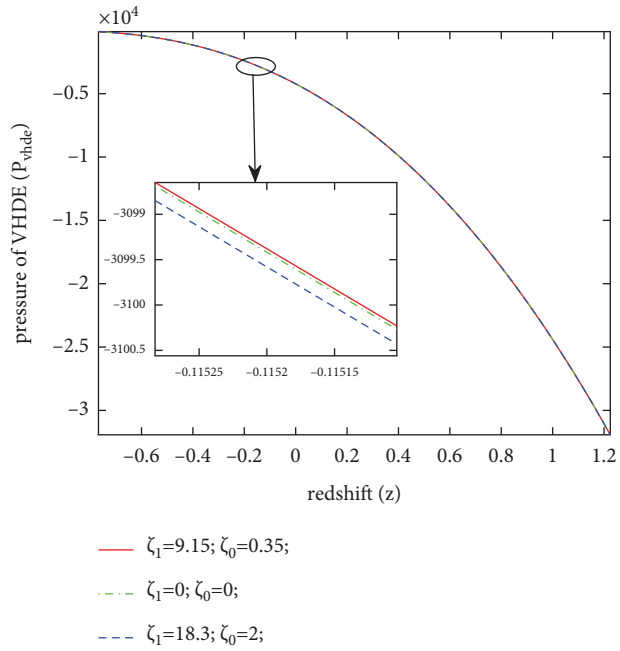

Figure 1: Pressure of VHDE (P_{vhde}) versus redshift (z) for BT-II.

$$\vartheta = \frac{2\dot{R}}{R} + \frac{\dot{S}}{S}, \tag{66}$$

whose expressions for the BT-II, VIII, and IX VHDE models are, respectively, given as

$$\begin{aligned} \vartheta &= \frac{\gamma_1 (2n+1)}{(2\beta_1 - 2\gamma_1 T)}, \\ \vartheta &= \gamma_2 \coth(2\gamma_2 T), \\ \&\quad \vartheta &= \gamma_3 \tanh(2\gamma_3 T). \end{aligned} \tag{67}$$

The shear scalar (σ^2) is defined by the following equation and is followed by the expressions of σ^2 for BT–II, VIII, and IX VHDE models, respectively, as

$$\sigma^2 = \frac{1}{2}\sigma^{ij}\sigma_{ij} = \frac{1}{2}\left(\sum_{i=1}^{3} H_i^2 - \frac{\vartheta^2}{3}\right), \tag{68}$$

$$\sigma^2 = \frac{\gamma_1^2 (2\beta_1 - 2\gamma_1 T)^{-2} (n-1)^2}{3}, \tag{69}$$

$$\sigma^2 = \frac{4\gamma_2^2 \coth^2(2\gamma_2 T)}{3}, \tag{70}$$

$$\&\sigma^2 = \frac{4\gamma_3^2 \tanh^2(2\gamma_3 T)}{3}. \tag{71}$$

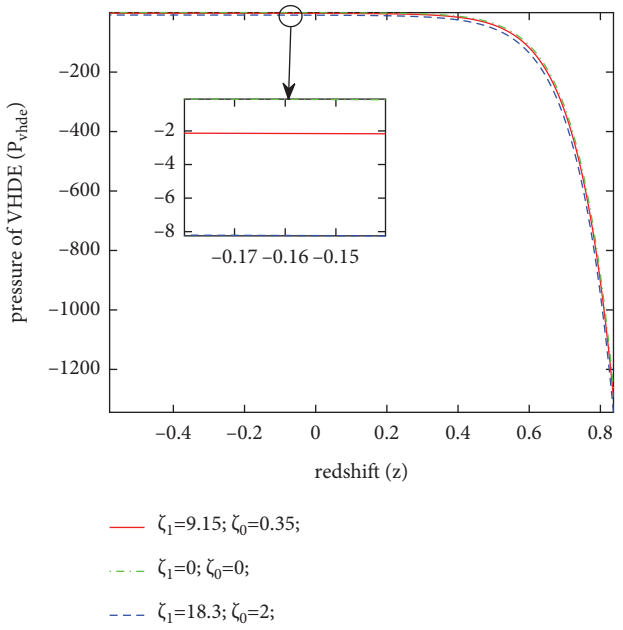

FIGURE 2: Pressure of VHDE (P_{vhde}) versus redshift for BT-VIII.

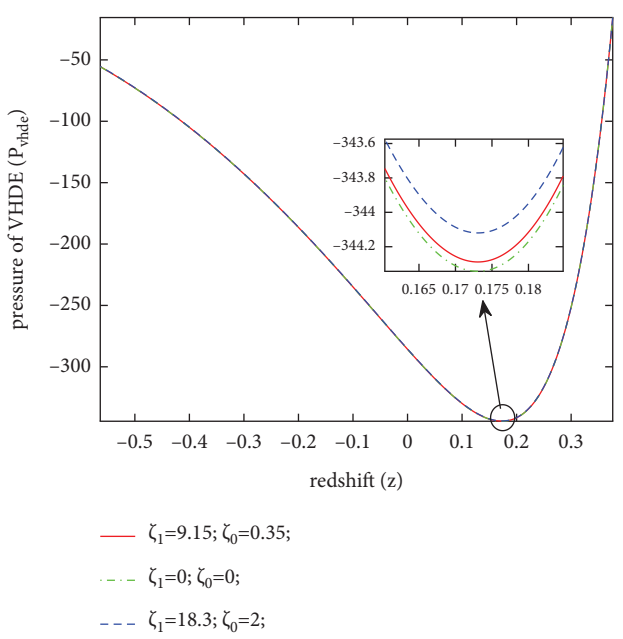

FIGURE 3: The pressure of VHDE(P_{vhde}) versus redshift (z) for BT-IX.

4. Some Other Important Properties of the Models

Now we compute the following dynamical parameters, which are significant in the physical discussion of the cosmological models presented in equations (35), (48), and (61).

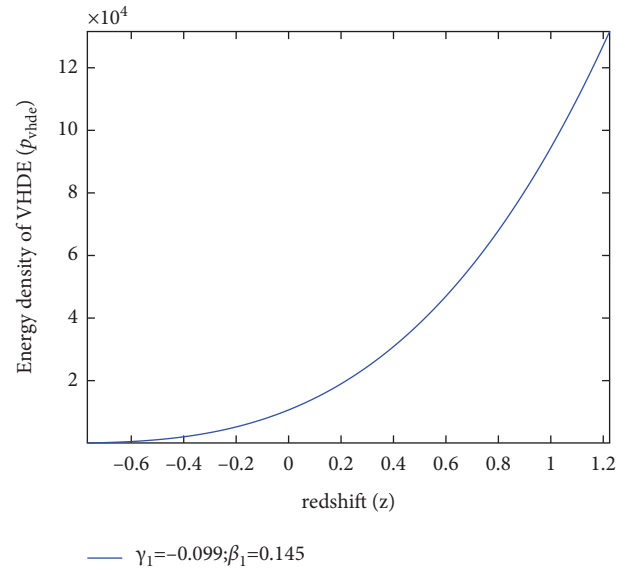

FIGURE 4: Energy density of VHDE (ρ_{vhde}) versus redshift (z) for BT-II.

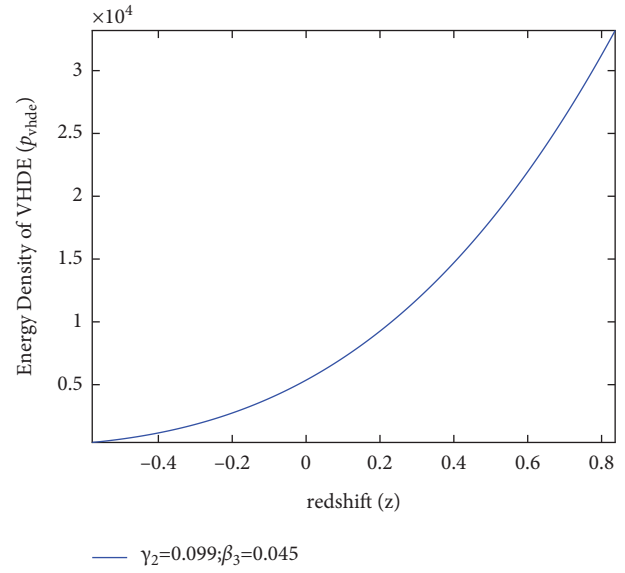

FIGURE 5: Energy density of VHDE (ρ_{vhde}) versus redshift (z) for BT-VIII.

4.1. Deceleration Parameter (q). The parameter is defined as

$$q = -\frac{a\ddot{a}}{\dot{a}^2}, \tag{72}$$

that depends upon the scale factor and its derivatives. It is considered to describe the transition phase of the Universe

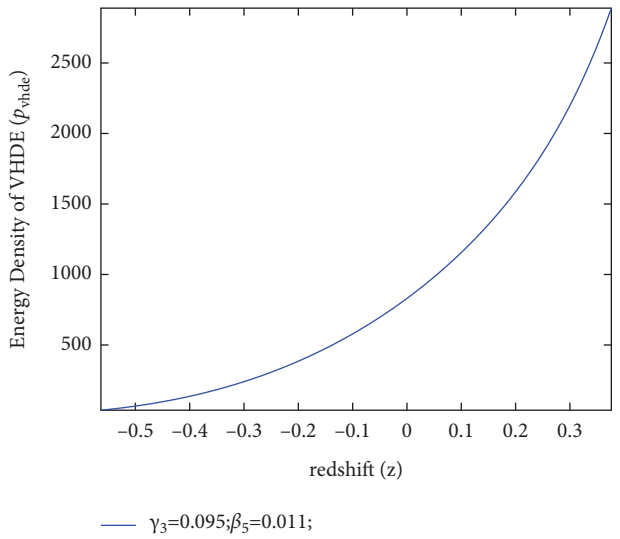

Figure 6: The energy density of VHDE (ρ_{vhde}) versus redshift (z) for BT-IX.

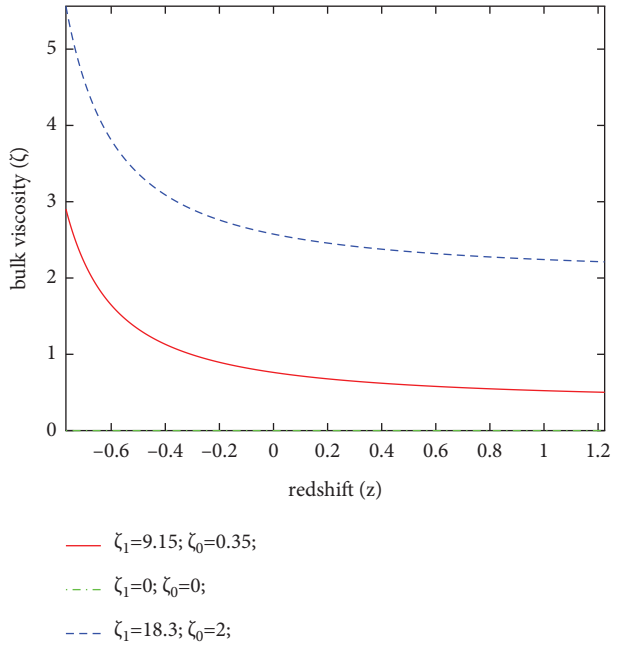

Figure 7: Bulk viscosity (ζ) versus redshift (z) for BT-II.

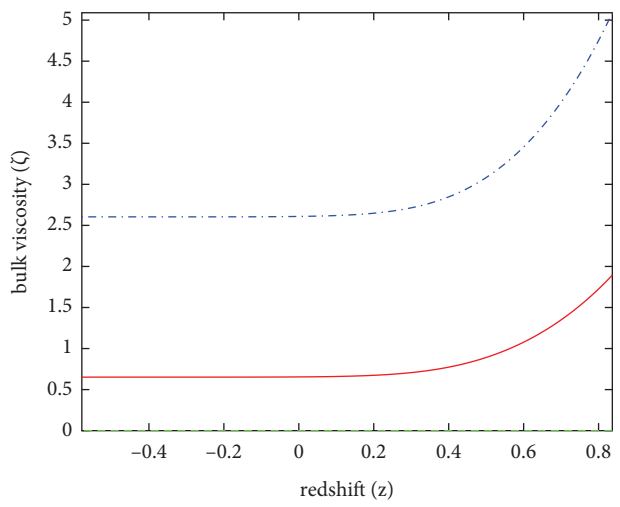

Figure 8: Bulk viscosity (ζ) versus redshift (z) for BT-VIII.

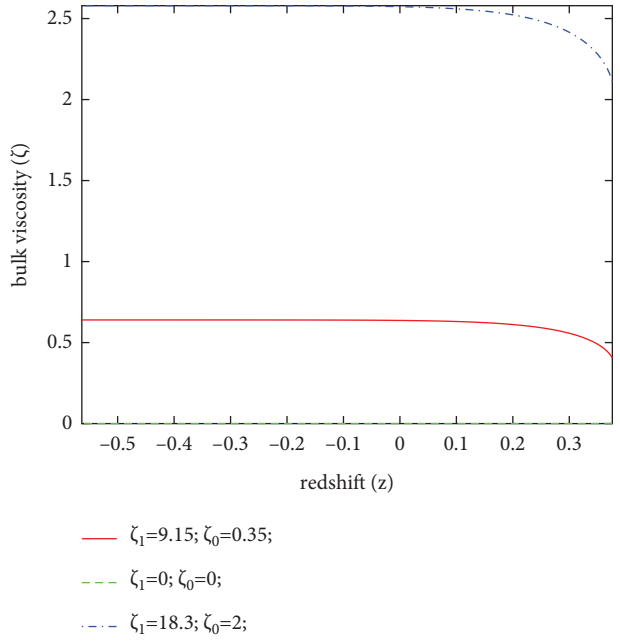

Figure 9: Bulk viscosity (ζ) versus redshift (z) for BT-IX.

and basically computes the expansion rate of the cosmos. Whenever the deceleration parameter shows a positive curve, it indicates the decelerated expansion of the Universe. Whereas, the negative curve implies that there is an accelerated expansion of the cosmos and at $q = 0$ there exists the marginal inflation. The deceleration parameters of the BT-II, VIII, and IX models are, respectively, given by

$$q = \frac{-6}{2n+1} - 1,$$
$$q = 6\text{sech}^2(2\gamma_2 T) - 1, \quad (73)$$
$$q = -6\text{cosech}^2(2\gamma_3 T) - 1.$$

The behavior of the deceleration parameter(q) for BT-VIII and IX models has been depicted against the redshift (z) in Figures 10 and 11, respectively. From Figure 10, it is observed that the path of the BT-VIII curve travels from the deceleration to the acceleration phase while passing through the transition line. Whereas, from Figure 11, it is clear that the curve for BT-IX varies in an accelerated phase. However, the deceleration parameter of BT-II is independent of time. Some of the authors, namely, Berman [107], Bishi et al. [108], Santhi et al. [109], Santhi and Naidu [110], Samanta [111], Kumar and Singh [112], have attained a constant q in their research.

4.2. Jerk Parameter (j)
The cosmic jerk,

$$j = \frac{1}{aH^3}\frac{d^3a}{dt^3}, \tag{74}$$

can be accounted for by the transition of the Universe from the decelerating to the accelerating phase. For various models of the cosmos, there is a variation in the transition of the Universe whenever the jerk parameter lies in the positive region and the deceleration parameter lies in the negative region (Visser [113]). Rapetti et al. [114] showed that for the flat ΛCDM model, the value of jerk becomes unity.

The Jerk parameter of the BT-II, VIII, and IX models is, respectively, given by

$$\begin{aligned} j &= \frac{4n + 40n + 91}{(2n+1)^2}, \\ j &= 54\text{sech}^2(2\gamma_2 T) + 1, \\ j &= 1 - 54\text{cosech}^2(2\gamma_3 T). \end{aligned} \tag{75}$$

Figures 12 and 13 represent the variations of the jerk parameter plotted against redshift (z) for the models BT-VIII and IX, respectively. The trajectory of the jerk parameter for the BT-VIII model in Figure 12 varies in the positive region, whereas for the BT-IX model in Figure 13, the trajectory varies in the negative region, both of which approach unity in late times. However, the jerk parameter for BT-II is independent of time. Santhi and Naidu [115], Rao et al. [116], Santhi et al. [117], Rao and Prasanthi [118], and Shaikh et al. [119] are some of the researchers who have acquired a constant jerk parameter in their work.

4.3. Statefinder Pair (r, s). As mentioned earlier, a mysterious force, the DE, may be responsible for the cosmos to undergo an accelerated expansion int the current era. But as of now, there is no adequate information about DE. Hence, it becomes necessary to identify and understand the various properties of DE and its importance in various kinds of cosmographic models. Ratra and Peebles [47], Kamenschik et al. [61], Armendariz Picon et al. [60] Dvali et al. [120] have proposed various studies to realize that different DE forms, such as quintessence, Chaplygin gas, k-essence, and brane world models, give several families of curves for scale factor $a(t)$. As a way of categorizing the various types of DE, Sahni et al. [121] have proposed a diagnostic pair known as the "statefinder diagnostic," defined as

$$r = \frac{\dddot{a}}{aH^3} \;\&\; s = \frac{r-1}{3(q-1/2)}, \tag{76}$$

that is based upon the derivatives of the scale factor $a(t)$ and the deceleration parameter q. We have obtained expressions for the statefinder diagnostic pair (r, s) for the models BT-II, VIII, and IX, which are respectively given by

$$\begin{aligned} r &= \frac{(2n+7)(2n+13)}{(2n+1)^2} \;\&\; s = \frac{-4}{(2n+1)}, \\ r &= 54\text{sech}^2(2\gamma_2 T) + 1 \;\&\; s = \frac{-12}{\cosh^2(2\gamma_2 T) - 4}, \\ \&\quad r &= 1 - 54\text{cosech}^2(2\gamma_3 T) \;\&\; s = \frac{12}{\cosh^2(2\gamma_3 T) + 3}. \end{aligned} \tag{77}$$

The interpretation of the statefinder pair from Figures 14 and 15 says that the (r, s) plane for BT–VIII and IX models starts its evolution from the quintessence and phantom regions and reaches the ΛCDM model(for $r = 1$, $s = 0$). Also, for the BT-II Universe, the statefinder plane is independent of time. Shanti et al. [122], Samanta and Mishra [123], Katore and Gore [124], and Shaikh et al. [119] are some of the authors who have obtained the statefinder parameters independent of time.

4.4. EoS Parameter (ω_{vhde}). To classify the phases of the inflating Universe, viz., the transition from decelerated to accelerated phases containing DE and radiation dominated eras, the EoS parameter (ω_{vhde}) can be broadly used, whose expression is given by $\omega_{vhde} = P_{vhde}/\rho_{vhde}$.

It categorizes various epochs as follows:

Decelerated phase:

(i) stiff fluid ($\omega_{vhde} = 1$),

(ii) the radiation dominated phase ($0 < \omega_{vhde} < 1/3$) and

(iii) dust fluid phase or cold dark matter ($\omega_{vhde} = 0$).

Accelerated phase:

(i) the quintessence phase ($-1 < \omega_{vhde} < -1/3$),

(ii) cosmological constant/vacuum phase ($\omega_{vhde} = -1$)

(iii) quintom era and phantom era ($\omega_{vhde} < -1$)

The EoS Parameter for the BT-II VHDE cosmological model is given by

$$\omega_{vhde} = \frac{\Upsilon_7}{\Upsilon_8}, \tag{78}$$

where

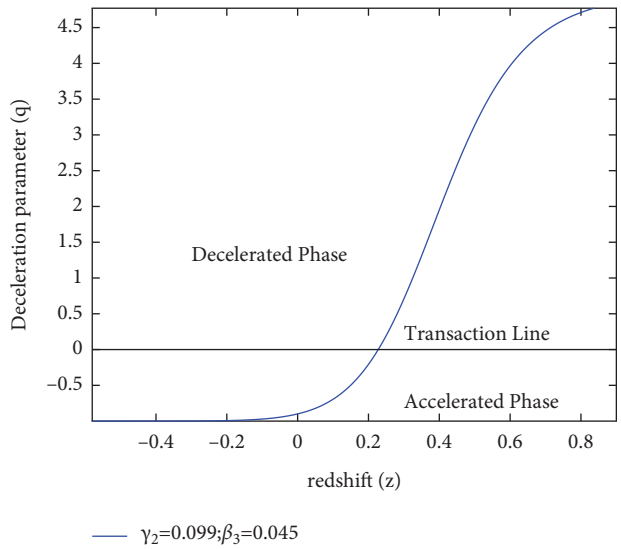

Figure 10: Deceleration parameter (q) versus redshift (z) for BT-VIII.

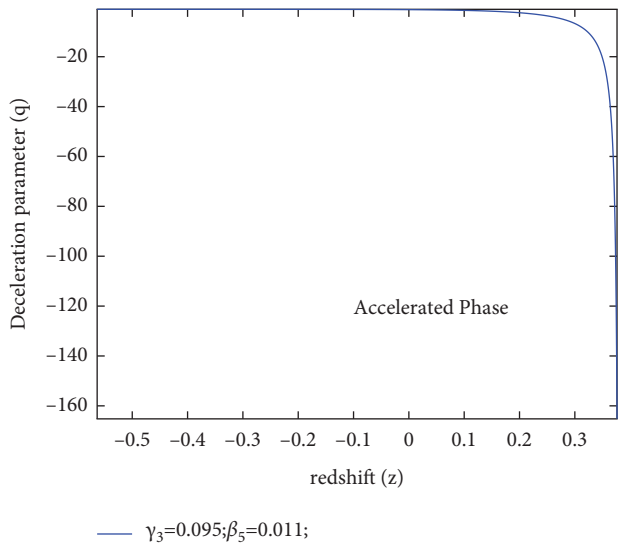

Figure 11: Deceleration parameter (q) versus redshift (z) for BT-IX.

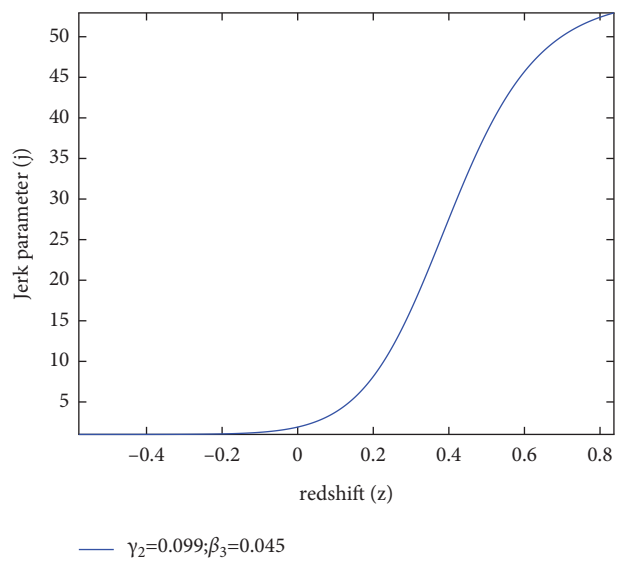

Figure 12: Jerk (j) versus redshift (z) for BT-VIII.

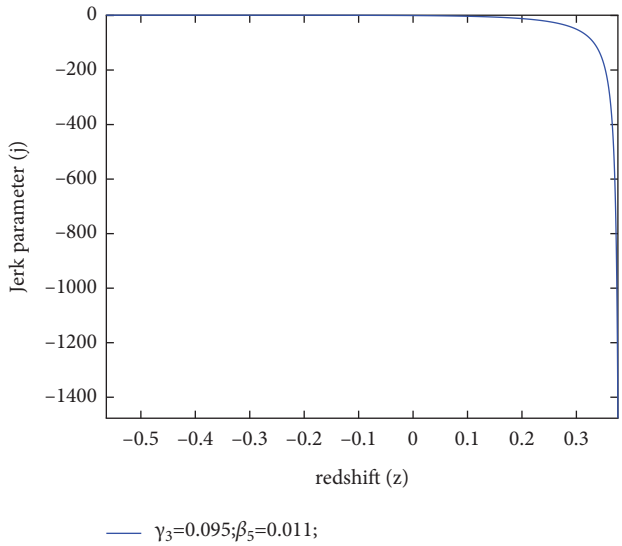

Figure 13: Jerk (j) versus redshift (z) for BT-IX.

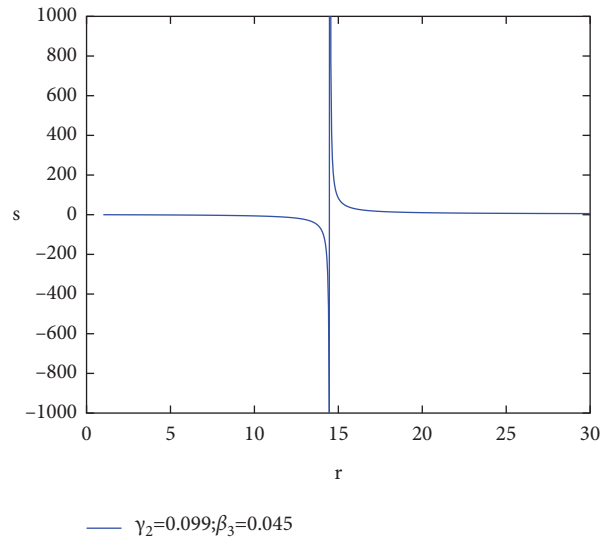

Figure 14: Statefinder plane ($r-s$) for BT-VIII.

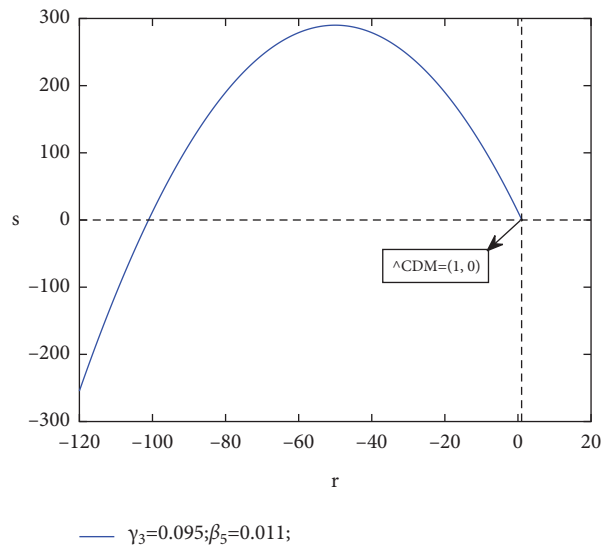

Figure 15: Statefinder plane ($r-s$) for BT-IX.

$$\Upsilon_7 = \frac{1}{576}\Bigg(-64\left(3+\left(n+\frac{1}{2}\right)m\right)(T\gamma_1-\beta_1)^3\gamma_1^2 m\left(n+\frac{1}{2}\right)(-2T\gamma_1+2\beta_1)^{\frac{(-2n-1)m+6n-12}{6}},$$

$$+144\gamma_1^2 n^2(T\gamma_1-\beta_1)^2(-2T\gamma_1+2\beta_1)^{\frac{(-2n-1)m+6n-6}{6}},$$

$$-8(T\gamma_1-\beta_1)\left(\frac{-27}{8}+\left(\left(n+\frac{1}{2}\right)^2\omega m^2+\left(-3n-\frac{3}{2}\right)m-\frac{27n^2}{2}+9n\right)\gamma_1^2\right)(-2T\gamma_1+2\beta_1)^{\frac{(-2n-1)m+6n}{6}},$$

$$+576(-2T\gamma_1+2\beta_1)^{-n}\pi\gamma_1\left(\left(T\zeta_0-\frac{\zeta_1 n}{3}-\frac{\zeta_1}{6}\right)\gamma_1-\zeta_0\beta_1\right)\left(n+\frac{1}{2}\right)\Bigg)\Bigg\}, \tag{79}$$

$$\Upsilon_8 = \Bigg((T\gamma_1-\beta_1)\left(\left(\frac{-1}{64}+\left(\frac{-1}{72}\left(n+\frac{1}{2}\right)^2\omega m^2+\frac{1}{12}\left(n+\frac{1}{2}\right)^2 m+\frac{n^2}{16}+\frac{n}{8}\right)\gamma_1^2\right)(-2T\gamma_1+2\beta_1)^{\frac{(-2n-1)m+6n}{6}},$$

$$+(-2T\gamma_1+2\beta_1)^{1/2}\pi\beta_2(T\gamma_1-\beta_1)\right)\Bigg)\Bigg\}.$$

The EoS parameter for the BT-VIII VHDE cosmological model is given by

$$\omega_{vhde} = \frac{\Upsilon_9}{\Upsilon_{10}}, \tag{80}$$

where

$$\Upsilon_9 = \Bigg(8\Bigg(\cosh^{m/3}(\theta)\left(\left(-18+\left(18+(\omega+2)m^2+6m\right)\gamma_2^2\right)\beta_3^2\cosh^4(T\gamma_2)-\left(-18+\left(18+(\omega+2)m^2+6m\right)\gamma_2^2\right)\beta_3^2\cosh^2(\gamma_2 T)+\frac{1}{4}\left(\frac{-27}{2}+\left(-54+(\omega+2)m^2-6m\right)\beta_3^2\right)\gamma_2^2\right)\left(\frac{\gamma_2}{\beta_3}\operatorname{cosech}(2\gamma_2 T)\right)^{-m/6}\Bigg\},$$

$$-96\left(\cosh^2(\gamma_2 T)-\frac{1}{2}\right)\pi\left(\gamma_2\cosh^2(\gamma_2 T)\sinh(\gamma_2 T)\zeta_1+3\cosh^3(\gamma_2 T)\zeta_0-\frac{\gamma_2}{2}\zeta_1\sinh(\gamma_2 T)-3\cosh(\gamma_2 T)\zeta_0\right)\cosh(\gamma_2 T)\beta_3^3\Big)\gamma_2\Bigg)$$

$$\Upsilon_{10} = \Bigg(1152\beta_4\cosh^3(\gamma_2 T)\sinh(\gamma_2 T)\pi\sqrt{2}\beta_3^3(\cosh(\gamma_2 T)-1)(\cosh(\gamma_2 T)+1)\left(\frac{\gamma_2}{\beta_3}\operatorname{cosech}(\gamma_2 T)\operatorname{sech}(\gamma_2 T)\right)^{1/2}$$

$$+8\cosh^{m/3}(\theta)\left(\left(18+\left(m^2\omega-6m+18\right)\gamma_2^2\right)\beta_3^2\cosh^4(\gamma_2 T)-\left(18+\left(m^2\omega-6m+18\right)\gamma_2^2\right)\beta_3^2\cosh^2(\gamma_2 T)+\frac{1}{4}\left(\frac{9}{2}+\left(m^2\omega-6m+18\right)\beta_3^2\right)\gamma_2^2\right)\left(\frac{\gamma_2}{\beta_3}\operatorname{cosech}(2\gamma_2 T)\right)^{-m/6}\gamma_2)\Bigg\}. \tag{81}$$

The EoS parameter for the BT-IX VHDE cosmological model is given by

$$\omega_{vhde} = \frac{\Upsilon_{11}}{\Upsilon_{12}}, \tag{82}$$

where

$$\Upsilon_{11} = \left(8\left(\sin^{\frac{m}{3}}(\theta)\left(\left(-18+\left(18+(\omega+2)m^2+6m\right)\gamma_3^2\right)\beta_5^2\cosh^4(\gamma_3 T)-\left(-18+\left(18+(\omega+2)m^2+6m\right)\gamma_3^2\right)\beta_5^2\cosh^2(\gamma_3 T)+\left(\frac{-27}{8}+(3m+18)\beta_5^2\right)\gamma_3^2-\frac{9\beta_5^2}{2}\right)\left(\frac{\gamma_3}{\beta_5}\operatorname{sech}(2\gamma_3 T)\right)^{-m/6}\right.\right.$$
$$\left.\left. -96\cosh(\gamma_3 T)\left(\gamma_3\cosh^3(\gamma_3 T)\zeta_1+3\cosh^2(\gamma_3 T)\sinh(\gamma_3 T)\zeta_0-\gamma_3\zeta_1\cosh(\gamma_3 T)-\frac{3\zeta_0}{2}\sinh(\gamma_3 T)\right)\pi\beta_5^3\left(\cosh^2(\gamma_3 T)-\frac{1}{2}\right)\right)\gamma_3\right),$$

$$\Upsilon_{12} = \left(2304\pi\beta_5^3\beta_6\left(\cosh^2(\gamma_3 T)-\frac{1}{2}\right)^3\left(\frac{\gamma_3}{\beta_5\left(2\cosh^2(\gamma_3 T)-1\right)}\right)^{1/2}+8\gamma_3\sin^{m/3}(\theta)\left(\frac{\gamma_3}{\beta_5}\operatorname{sech}(2\gamma_3 T)\right)^{-m/6}\left(\left(-18+\left(m^2\omega-6m+18\right)\gamma_3^2\right)\beta_5^2\cosh^4(\gamma_3 T)\right.\right.$$
$$\left.\left. -\left(-18+\left(m^2\omega-6m+18\right)\gamma_3^2\right)\beta_5^2\cosh^2(\gamma_3 T)+\frac{9\gamma_3^2}{8}-\frac{9\beta_5^2}{2}\right)\right)\right\}. \tag{83}$$

Figures 16–18 show the behavior of the EoS parameter (ω_{vhde}) taken against redshift (z) with different values of ζ_0 and ζ_1 for all the three models of BT-II, VIII, and IX, respectively. Here, we notice that the curves of ω_{vhde} for BT-II and IX models for different values of ζ_0 and ζ_1 begin from the quintessence region ($-1 < \omega_{vhde} < -1/3$) and cross the nonrelativistic matter ($\omega_{vhde} = -1$) then reaching the phantom region ($\omega_{vhde} < -1$), whereas for BT-VIII, in the presence of null viscosity (*i.e.*, $\zeta_0 = 0$ and $\zeta_1 = 0$), the curve of ω_{vhde} varies in the quintessence region and as the values of ζ_0 and ζ_1 are increased, we get the quintessence to the phantom region by crossing the phantom divided line, varying more in the phantom region, which indicates accelerated expansion of the Universe. According to the obtained models, the observed EoS parameters match the 2018 Planck data [125], where the EoS parameter limits are as follows:

$$\omega_{vhde} = \begin{cases} -1.56^{+0.60}_{-0.48}\,(\text{Planck} + \text{TT} + \text{loE}), \\ -1.58^{+0.52}_{-0.41}\,(\text{Planck} + \text{TT}, \text{EE} + \text{loE}), \\ -1.57^{+0.50}_{-0.40}\,(\text{Planck} + \text{TT}, \text{TE}, \text{EE} + \text{loE} + \text{lensing}), \\ -1.04^{+0.10}_{-0.10}\,(\text{Planck} + \text{TT}, \text{TE}, \text{EE} + \text{loE} + \text{lensing} + \text{BAO}). \end{cases} \tag{84}$$

4.5. $\omega_{vhde} - \omega_{vhde}'$ plane. Cadwell and Linder [126] have suggested $\omega_{vhde} - \omega_{vhde}'$ plane (where ' signifies differentiation w.r.t ln a) to interpret the accelerated expansion regions of the cosmos and to analyze the quintessence scalar field for the first time. For various values of ω_{vhde} and ω_{vhde}', the plane describes two distinct areas. The plane is described as the thawing zone for $\omega_{vhde}' > 0$ when $\omega_{vhde} < 0$ and the freezing region for $\omega_{vhde}' < 0$ when $\omega_{vhde} < 0$.

For the BT-II VHDE cosmological model,

$$\omega' = \frac{\Upsilon_{13}}{\Upsilon_{14}}, \tag{85}$$

where

$$\Upsilon_{13} = \frac{1}{36}\left(\pi\left(8\left(3+\left(n+\frac{1}{2}\right)m\right)\left(\left(n+\frac{1}{2}\right)m-3n+\frac{9}{2}\right)(T\gamma_1-\beta_1)^5\beta_2\left(n+\frac{1}{2}\right)\gamma_1^2 m(-2T\gamma_1+2\beta_1)^{((2n-1)m+6n-15/6)}-18n^2\left(\left(n+\frac{1}{2}\right)m-3n+\frac{9}{2}\right)(T\gamma_1-\beta_1)^4\beta_2\gamma_1^2(-2T\gamma_1+2\beta_1)^{((-2n-1)m+6n-9/6)}\right.\right.$$
$$+\frac{1}{2}\left(n+\frac{1}{2}\right)\gamma_1\left(\left(n+\frac{1}{2}\right)^2\gamma_2^1\omega m^2-6\left(n+\frac{1}{2}\right)^2\gamma_1^2 m-\frac{9\gamma_1^2 n^2}{2}-9\gamma_1^2 n+\frac{9}{8}\right)\left(\left(n+\frac{1}{2}\right)\left(\frac{-\gamma_1\zeta_1 n}{3}+\left(T\zeta_0-\frac{\zeta_1}{6}\right)\gamma_1-\zeta_0\beta_1\right)m+2n^2\zeta_1\gamma_1+((-6T\zeta_0+2\zeta_1)\gamma_1+6\zeta_0\beta_1)n+\frac{\gamma_1\zeta_1}{2}\right)(-2T\gamma_1+2\beta_1)^{(-2nm-m/6)}$$
$$\left.\left.+(T\gamma_1-\beta_1)^2\beta_2\left(-216\left(\frac{-n^2\zeta_1\gamma_1}{3}+((T\zeta_0-\zeta_1)\gamma_1-\zeta_0\beta_1)n+\left(\frac{3T\zeta_0}{2}-\frac{5\zeta_1}{12}\right)\gamma_1-\frac{3T\zeta_0\beta_1}{2}\right)\pi\left(n+\frac{1}{2}\right)\gamma_1(-2T\gamma_1+2\beta_1)^{-n-(1/2)}+\left(\left(n+\frac{1}{2}\right)m-3n+\frac{9}{2}\right)(T\gamma_1-\beta_1)(-2T\gamma_1+2\beta_1)^{((-2n-1)m+6n-3/6)}\left(\left(n+\frac{1}{2}\right)^2\gamma_2^1\omega m^2-3\left(n+\frac{1}{2}\right)\gamma_2^1 m-\frac{27}{8}-\frac{27\gamma_2^1 n^2}{2}+9\gamma_2^1 n\right)\right)\right)\right),$$

$$\Upsilon_{14} = \left((T\gamma_1-\beta_1)\left(\left(\frac{-1}{72}\left(n+\frac{1}{2}\right)^2\gamma_1^2\omega m^2+\frac{1}{12}\left(n+\frac{1}{2}\right)^2\gamma_1^2 m+\frac{\gamma_1^2 n^2}{16}+\frac{\gamma_1^2 n}{8}-64\right)(-2T\gamma_1+2\beta_1)^{(-2n-1)m+6n/6}+(-2T\gamma_1+2\beta_1)^{1/2}\pi\beta_2(T\gamma_1-\beta_1)\right)^2\left(n+\frac{1}{2}\right)\right).\Bigg\} \tag{86}$$

For the BT-VIII VHDE cosmological model,

$$\omega'_{vhde} = \frac{\Upsilon_{15}}{\Upsilon_{16}}, \tag{87}$$

where

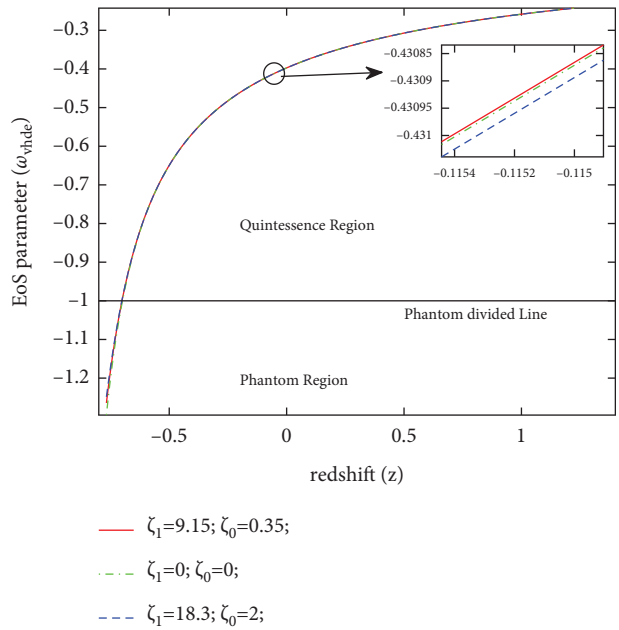

Figure 16: EoS parameter (ω_{vhde}) versus redshift (z) for BT-II.

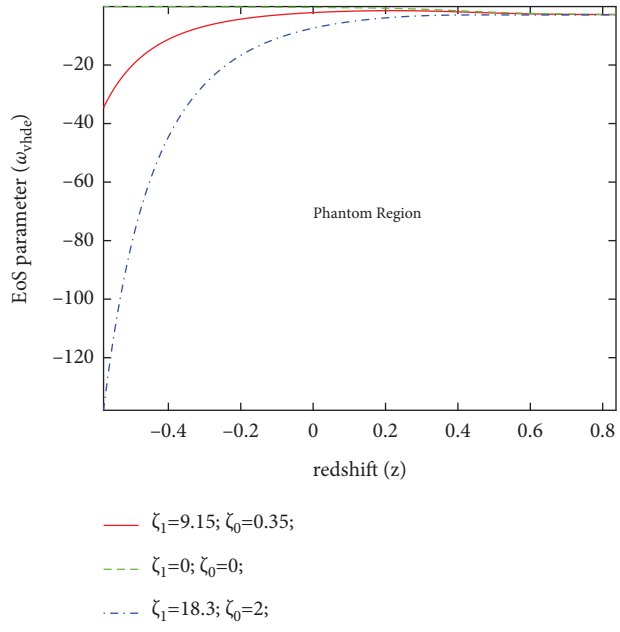

Figure 17: EoS parameter $(\omega_{vhde})(\omega_{vhde})$ versus redshift (z) for BT-VIII.

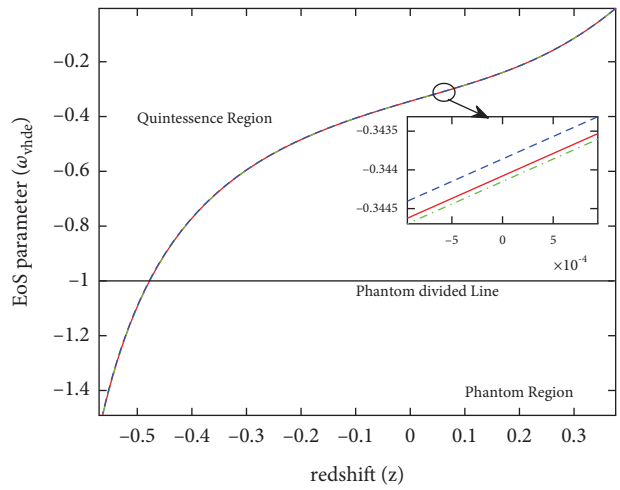

Figure 18: EoS parameter versus redshift (z) for BT-IX.

$$\Upsilon_{16}=\left(\frac{\gamma_2}{\beta_3}\cos ech(2\gamma_2T)\right)^{(1/2)}\left(\beta_4\cosh^3(\gamma_2T)\sinh(\gamma_2T)\pi\sqrt{2}\,\beta_3^3\left(\cosh^2(\gamma_2T)-1\right)\left(\frac{\gamma_2}{\beta_3}\operatorname{cosech}(\gamma_2T)sech(\gamma_2T)\right)^{(1/2)}+\frac{\cosh^{(m/3)}(\theta)}{144}\right.$$
$$\left.\left(\left(18+\left(m^2\omega-6m+18\right)\gamma_2^2\right)\beta_3^2\cosh^4(\gamma_2T)-\left(18+\left(m^2\omega-6m+18\right)\gamma_2^2\right)\beta_3^2\cosh^2(\gamma_2T)+\frac{1}{4}\left(\frac{9}{2}+\left(m^2\omega-6m+18\right)\beta_3^2\right)\gamma_2^2\right)\left(\frac{\gamma_2}{\beta_3}\operatorname{cosech}(2\gamma_2T)\right)^{(-m/6)}\gamma_2^2\cosh(2\gamma_2T)\right)\Bigg\},$$

$$\Upsilon_{15}=\frac{1}{144}\left\{\begin{array}{l}\left(\frac{\sqrt{2}}{8}\frac{8}{3}\cosh^{(m/3)}(\theta)\pi\zeta_1(m-6)\left(18+\left(m^2\omega-6m+18\right)\gamma_2^2\right)\beta_3^2\gamma_2\cosh^{10}(\gamma_2T)+3\zeta_0(m-6)\sinh(\gamma_2T)\left(18+\left(m^2\omega-6m+18\right)\gamma_2^2\right)\beta_3^2\cosh^9(\gamma_2T)-\frac{5\zeta_1}{2}(m-6)\left(18+\left(m^2\omega-6m+18\right)\gamma_2^2\right)\beta_3^2\gamma_2\cosh^8(\gamma_2T)-6\zeta_0(m-6)\sinh(\gamma_2T)\left(18+\left(m^2\omega-6m+18\right)\gamma_2^2\right)\right.\\ \beta_3^2\cosh^7(\gamma_2T)+\frac{5\zeta_1}{2}\left(\left((m-6)\left(m^2\omega-6m+18\right)\gamma_2^2+\frac{81m}{5}-\frac{378}{5}\right)\beta_3^2+\frac{9\gamma_2^2}{20}(m-18)\right)\gamma_2\cosh^6(\gamma_2T)+\frac{9\zeta_0}{2}\sinh(\gamma_2T)\left(\left((m-7)\left(m^2\omega-6m+18\right)\gamma_2^2+15m-72\right)\beta_3^2+\frac{3\gamma_2^2}{4}(m-18)\right)\\ \cosh^5(\gamma_2T)-\frac{5\zeta_1}{4}\left(\left((m-6)\left(m^2\omega-6m+18\right)\gamma_2^2+\frac{63m}{5}-\frac{54}{5}\right)\beta_3^2+\frac{27\gamma_2^2}{20}(m-18)\right)\gamma_2\cos^4(\gamma_2T)-\frac{3\zeta_0}{2}\sinh(\gamma_2T)\left(\left((m-9)\left(m^2\omega-6m+18\right)\gamma_2^2+9m\right)\beta_3^2+\frac{9\gamma_2^2}{4}(m-18)\right)\\ \cosh^3(\gamma_2T)+\frac{5\zeta_1}{16}\left(\left((m-6)\left(m^2\omega-6m+18\right)\gamma_2^2+\frac{36m}{5}+\frac{216}{5}\right)\beta_3^2\frac{27\gamma_2^2}{10}(m-14)\right)\gamma_2\cosh^2(\gamma_2T)+\frac{3\zeta_0}{16}(m-12)\sinh(\gamma_2T)\left(\frac{9}{2}+\left(m^2\omega-6m+18\right)\beta_3^2\right)\gamma_2^2\cosh(\gamma_2T)-\frac{\zeta_1}{32}(m-6)\left(\frac{9}{2}+\left(m^2\omega-6m+18\right)\beta_3^2\right)\gamma_2^3\\ \beta_3\left(\frac{\gamma^2}{\beta_3}\cos ech(2\gamma_2T)\right)^{(-m/6)}+\left(\cosh^2(\gamma_2T)-\frac{1}{2}\right)\cosh^{(2m/3)}(\theta)\left(\frac{\gamma_2}{\beta_3}\cos ech(2\gamma_2T)\right)^{(-m/3)}\sinh(\gamma_2T)\gamma_2^2\left(\left((m+6)\left(m^2\omega-6m+18\right)\gamma_2^2+54(-3\omega-3)m^2+18m\right)\beta_3^2+\frac{27}{2}+\left(27+\left(\frac{3\omega}{2}+\frac{3}{4}\right)m^2-\frac{9m}{2}\right)\gamma_2^2\right)\cosh(\gamma_2T)\left(\frac{\gamma_2}{\beta_3}\cos ech(\gamma_2T)sech(\gamma_2T)\right)^{(1/2)}\\ +\beta_4\pi\left(\cosh^{m/3}(\theta)\left(\cosh^2(\gamma_2T)-\frac{1}{2}\right)\left(\left(-18+\left(18+(\omega+2)m^2+6m\right)\gamma_2^2\right)(m-3)\beta_3^2\cosh^4(\gamma_2T)-\left(-18+\left(18+(\omega+2)m^2+6m\right)\gamma_2^2\right)(m-3)\beta_3^2\cosh^2(\gamma_3T)+\frac{1}{4}\left(\frac{-27}{2}+\left(-54+(\omega+2)m^2-6m\right)\beta_3^2\right)(m-15)\gamma_2^2\right)\sinh(\gamma_2T)\left(\frac{\gamma_2}{\beta_3}\cos eh(2\gamma_2T)\right)^{-m/6}\right)\\ -288\left(\cosh(\gamma_2T)+1\right)\left(\gamma_2\cosh^6(\gamma_2T)\zeta_1+3\cosh^5(\gamma_2T)\sinh(\gamma_2T)\zeta_0-\frac{3\gamma_2}{2}\cosh^4(\gamma_2T)\zeta_1-3\cosh^3(\gamma_2T)\sinh(\gamma_2T)\zeta_0-\frac{\gamma_2\zeta_1}{4}\cosh^2(\gamma_2T)-\frac{3}{4}\cosh(\gamma_2T)\sinh(\gamma_2T)\zeta_0+\frac{3\zeta_1\gamma_2}{8}\right)\pi\left(\cosh(\gamma_2T)-1\right)\beta_3^3\cosh(\gamma_2T)\cosh(\gamma_2T)\sinh(2\gamma_2T)\beta_3^2\gamma_2^2\end{array}\right\}. \tag{88}$$

For the BT-IX VHDE cosmological model,

$$\omega'_{vhde}=\frac{\Upsilon_{17}}{\Upsilon_{18}}, \tag{89}$$

where

$$\Upsilon_{17} = -\Big(36\gamma_3\beta_5^2\cosh(2\gamma_3T)\Big(\Big(\frac{-8}{3}\Big(3\big(-18+\big(m^2\omega-6m+18\big)\gamma_3^2\big)\beta_5^2\varsigma_0(m-6)\cosh^{10}(\gamma_3T)+\varsigma_1\big(-18+\big(m^2\omega-6m+18\big)\gamma_3^2\big)\gamma_3\beta_5^2(m-6)\sinh(\gamma_3T)\cosh^9(\gamma_3T)-\frac{15}{2}\big(-18+\big(m^2\omega-6m+18\big)\gamma_3^2\big)$$
$$\beta_5^2\varsigma_0(m-6)\cosh^8(\gamma_3T)-2\varsigma_1\big(-18+\big(m^2\omega-6m+18\big)\gamma_3^2\big)\gamma_3\beta_5^2(m-6)\sinh(\gamma_3T)\cosh^7(\gamma_3T)+6\varsigma_0\Big(\Big(\Big(m-\frac{21}{4}\Big)\big(m^2\omega-6m+18\big)\gamma_3^2-\frac{81m}{4}+135\Big)\beta_5^2+\frac{9\gamma_3^2}{16}(m-18)\Big)\cosh^6(\gamma_3T)+$$
$$\Big(\big((m-16)\big(m^2-6m+18\big)\gamma_3^2-\frac{45m}{2}+189\big)\beta_5^2+\frac{9\gamma_3^2}{8}(m-18)\Big)\varsigma_1\gamma_3\sinh(\gamma_3T)\cosh^5(\gamma_3T)-\frac{3}{2}\Big(\Big(\big(m^2\omega-6m+18\big)\Big(m-\frac{3}{2}\Big)\gamma_3^2-\frac{63m}{2}+270\Big)\beta_5^2+\frac{27\gamma_3}{8}(m-18)\Big)\varsigma_0\cosh^4(\gamma_3T)$$
$$-\frac{9\varsigma_0}{8}\gamma_3\sinh(\gamma_3T)(\gamma_3-2\beta_5)(\gamma_3+2\beta_5)(m-18)\cosh^3(\gamma_3T)+\frac{9}{4}\Big(\big(\big(m^2\omega-6m+18\big)\gamma_3^2-3m+45\big)\beta_5^2+\frac{3\gamma_3^2}{4}(m-21)\Big)\varsigma_0\cosh^2(\gamma_3T)-\frac{27}{8}\varsigma_1\gamma_3\sinh(\gamma_3T)(\gamma_3-2\beta_5)(\gamma_3+2\beta_5)\cosh(\gamma_3T)$$
$$+\frac{81\varsigma_0\gamma_3^2}{32}-\frac{81\beta_5^2\varsigma_0}{8}\pi\beta_5\sin^{(m/3)}(\theta)\Big(\frac{\gamma_3}{\beta_5}\operatorname{sech}(2\gamma_3T)\Big)^{(-m/6)}+\Big(\frac{\gamma_3}{\beta_5}\operatorname{sech}(2\gamma_3T)\Big)^{(-m/3)}\Big(\big(\big(m^2\omega-6m+18\big)\gamma_3^2+3m-18\big)(m+6)\beta_5^2+27+\Big(-27+\Big(\frac{-3\omega}{2}-\frac{3}{4}\Big)m^2+\frac{9m}{2}\Big)\gamma_3^2\Big)\sin^{(2m/3)}(\theta)\cosh(\gamma_3T)\Big(\cosh^2(\gamma_3T)-\frac{1}{2}\Big)\gamma_3^2\sinh(\gamma_3T)$$
$$\Big(\frac{\gamma_3}{\beta_5\big(2\cosh^2(\gamma_3T)-1\big)}\Big)^{(1/2)}-4\pi\Big(\cosh^2(\gamma_3T)-\frac{1}{2}\Big)\beta_6\cosh(\gamma_3T)\Big(\big(-18+\big(18+(\omega+2)m^2+6m\big)\gamma_3^2\big)(m-3)\beta_5^2\cosh^4(\gamma_3T)-\big(-18+\big(18+(\omega+2)m^2+6m\big)\gamma_3^2\big)(m-3)\beta_5^2\cosh^2(\gamma_3T)+\Big(\big(-216+(3\omega+9)m^2-9m\big)\gamma_3^2-\frac{9m}{2}+\frac{27}{2}\Big)\beta_5^2-\frac{27\gamma_3^2}{8}(m-15)\Big)$$
$$\sin^{(m/3)}(\theta)\sinh(\gamma_3T)\Big(\frac{\gamma_3}{\beta_5}\cosh(2\gamma_3T)\Big)^{(-m/6)}-288\Big(\gamma_3\cosh^5(\gamma_3T)\sinh(\gamma_3T)\varsigma_1+3\varsigma_0\cosh^6(\gamma_3T)-\gamma_3\cosh^3(\gamma_3T)\sinh(\gamma_3T)\varsigma_1-\frac{9\varsigma_0}{2}\cosh^4(\gamma_3T)+\gamma_3\cosh(\gamma_3T)\sinh(\gamma_3T)\varsigma_1+3\varsigma_0\cosh^2(\gamma_3T)-\frac{3\varsigma_0}{4}\Big)\pi\Big(\cosh^2(\gamma_3T)-\frac{1}{2}\Big)\beta_5^2\Big)\Big)\Big)\Big)$$

$$\Upsilon_{18} = \Big(\Big(\Big(\sin^{2m/3}(\theta)\Big(\big(-18+\big(m^2\omega-6m+18\big)\gamma_3^2\big)\beta_5^2\cosh^4(\gamma_3T)-\big(-18+\big(m^2\omega-6m+18\big)\gamma_3^2\big)\beta_5^2\cosh^2(\gamma_3T)+\frac{9\gamma_3^2}{8}-\frac{9\beta_5^2}{2}\Big)\gamma_3\Big(\frac{\gamma_3}{\beta_5}\operatorname{sech}(2\gamma_3T)\Big)^{-m/3}+41472\pi^2\Big(\cosh^2(\gamma_3T)-\frac{1}{2}\Big)^5\beta_5^2\beta_6^4\Big)$$
$$\Big(\frac{\gamma_3}{\beta_5\big(2\cosh^2(\gamma_3T)-1\big)}\Big)^{1/2}+288\pi\Big(\cosh^2(\gamma_3T)-\frac{1}{2}\Big)\Big(\big(-18+\big(m^2\omega-6m+18\big)\gamma_3^2\big)\beta_5^2\cosh^4(\gamma_3T)-\big(-18+\big(m^2\omega-6m+18\big)\gamma_3^2\big)\beta_5^2\cosh^2(\gamma_3T)+\frac{9\gamma_3^2}{8}-\frac{9\beta_5^2}{2}\Big)\Big(\frac{\gamma_3}{\beta_5}\operatorname{sech}(2\gamma_3T)\Big)^{-m/6}\gamma_3\beta_5^2\sin^{m/3}(\theta)\beta_6\Big)\sinh(2\gamma_3T)\Big)\Big\}. \tag{90}$$

The evolutionary trajectories of $\omega_{vhde}-\omega_{vhde}'$ plane for the BT–II, VIII, and IX models are plotted with different values of ζ_0 and ζ_1 in Figures 19–21, respectively and we notice that the $\omega_{vhde}-\omega_{vhde}'$ plane for the BT-II and IX models vary in the freezing region (*i.e.*, $\omega_{vhde}<0$ and $\omega_{vhde}'<0$) whereas, the $\omega_{vhde}-\omega_{vhde}'$ plane of the BT-VIII model varies in thawing region (*i.e.*, $\omega_{vhde}<0$ and $\omega_{vhde}'>0$) for small values of ζ_0 and ζ_1. However, by increasing the values of ζ_0 and ζ_1 we get the freezing region for the BT-VIII model. Hence, the $\omega_{vhde}-\omega_{vhde}'$ plane of our obtained models is in accordance with the present observational data [127, 128] as follows:

$$\begin{aligned}
&\omega_{vhde} = -1.17^{+0.13}_{-0.12},\\
&\omega'_{vhde} = 0.85^{+0.50}_{-0.49}\,(\mathrm{WMAP}+\mathrm{eCAMB}+\mathrm{BAO}+\mathrm{H}_0+\mathrm{SNe}),\\
&\omega_{vhde} = -1.13^{+0.24}_{-0.25},\\
&\omega'_{vhde} < 1.32\,(\mathrm{Planck}+\mathrm{WP}+\mathrm{BAO}),\\
&\omega_{vhde} = -1.34^{+0.18}_{-0.18},\\
&\omega'_{vhde} = 0.85\pm0.7\,(\mathrm{WMAP}+\mathrm{eCAMB}+\mathrm{BAO}+\mathrm{H}_0).
\end{aligned} \tag{91}$$

4.6. Stability of the Model. To examine the stability of any DE model, we utilize the squared speed of sound (v_s^2). The models with $v_s^2<0$ shows instability where as models with $v_s^2>0$ shows stability. Hence, the v_s^2 is determined as follows [129]:

$$v_s^2 = \frac{P'_{vhde}}{\rho'_{vhde}}, \tag{92}$$

where P_{vhde}' and ρ_{vhde}' are the differentiation of pressure and density of VHDE w.r.t cosmic time 'T', respectively.

The squared speed of the sound for the BT-II VHDE model is given by

$$v_s^2 = \frac{\Upsilon_{19}}{\Upsilon_{20}}, \tag{93}$$

where

$$\begin{aligned}
\Upsilon_{19} = \frac{-1}{54}\Big(\Big(&(T\gamma_1-\beta_1)^3\Big(\Big(n+\frac{1}{2}\Big)m-6n+3\Big)\gamma_1^2\Big(n+\frac{1}{2}\Big)m\Big(3+\Big(n+\frac{1}{2}\Big)m\Big)(-2T\gamma_1+2\beta_1)^{((-2n-1)m+6n-12)/6},\\
&-\frac{9n^2}{4}(T\gamma_1-\beta_1)^2\Big(\Big(n+\frac{1}{2}\Big)m-6n+3\Big)\gamma_1^2(-2T\gamma_1+2\beta_1)^{((-2n-1)m+6n-6)/6}+\frac{1}{8}(T\gamma_1-\beta_1)\Big(\Big(n+\frac{1}{2}\Big)m-6n+3\Big),\\
&\Big(\frac{-27}{8}+\Big(\Big(n+\frac{1}{2}\Big)^2\omega m^2+\Big(-3n-\frac{3}{2}\Big)m-\frac{27n^2}{2}+9n\Big)\gamma_1^2\Big)(-2T\gamma_1+2\beta_1)^{((-2n-1)m+6n)/6},\\
&-27(-2T\gamma_1+2\beta_1)^{-n}\pi\gamma_1\Big(n+\frac{1}{2}\Big)\Big(\Big(T\zeta_0-\frac{2n\zeta_1}{3}-\frac{\zeta_1}{3}\Big)\gamma_1-\zeta_0\beta_1\Big)\Big)(-2T\gamma_1+2\beta_1)^{1/2}\Big)\Big\},\\
\Upsilon_{20} = \Big((T\gamma_1-\beta_1)\Big(&\frac{-1}{432}\Big(\Big(n+\frac{1}{2}\Big)m-6n+3\Big)\Big(\frac{9}{8}+\Big(\Big(n+\frac{1}{2}\Big)^2\omega m^2-6\Big(n+\frac{1}{2}\Big)^2m-\frac{9n^2}{2}-9n\Big)\gamma_1^2\Big),\\
&(-2T\gamma_1+2\beta_1)^{((-2m+6)n-m+3)/6}+(T\gamma_1-\beta_1)^2\pi\beta_2\Big(n+\frac{1}{2}\Big)\Big)\Big)\Big\}.
\end{aligned} \tag{94}$$

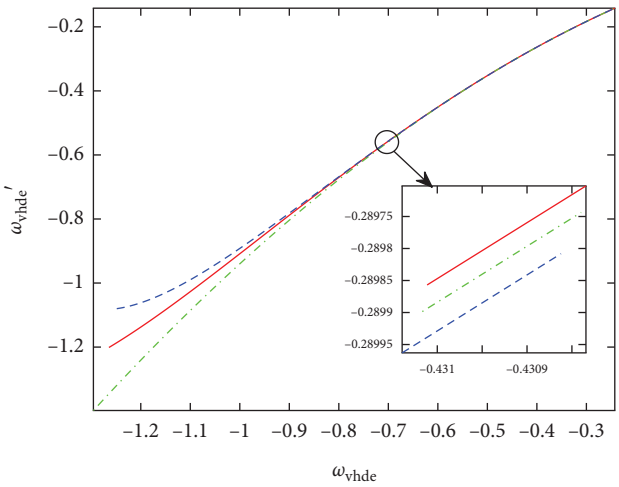

Figure 19: EoS plane $(\omega_{vhde} - \omega_{vhde}')$ for BT-II.

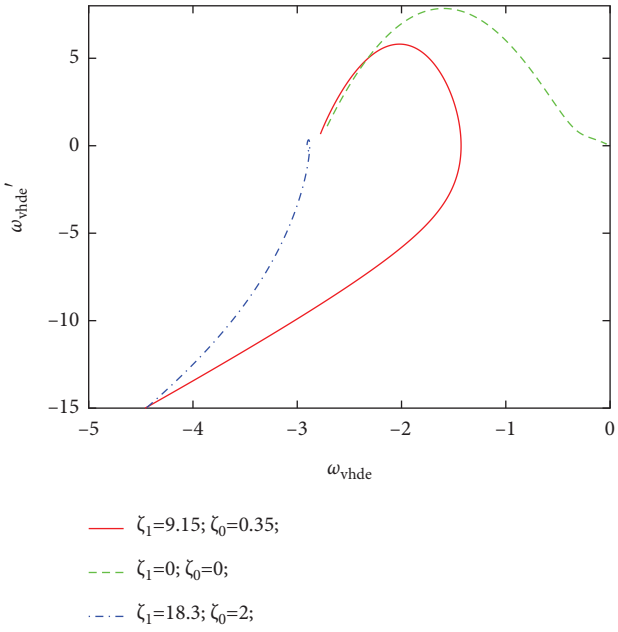

Figure 20: EoS plane $(\omega_{vhde} - \omega_{vhde}')$ for BT-VIII.

For the BT-VIII VHDE cosmological model, where

$$v_s^2 = \frac{\Upsilon_{21}}{\Upsilon_{22}}, \tag{95}$$

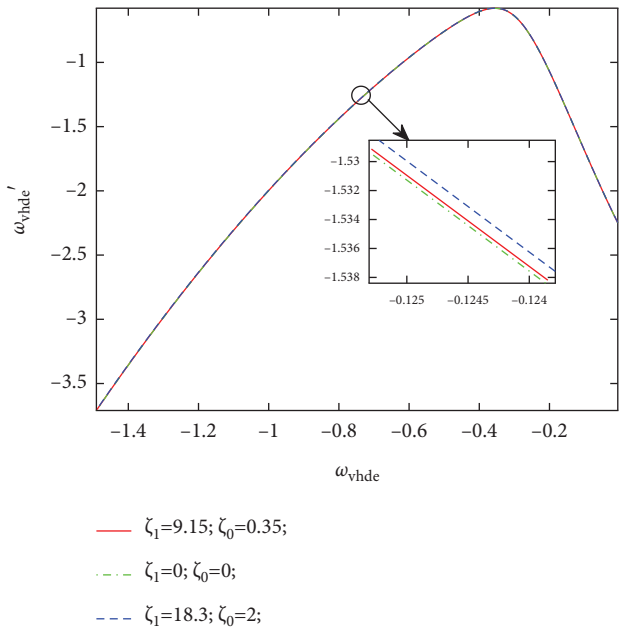

Figure 21: EoS plane $(\omega_{vhde} - \omega_{vhde}')$ for BT-IX.

$$\begin{aligned}
\Upsilon_{21} = &\left(4\left(\cosh^{(m/3)}(\theta)\left(\cosh^2(\gamma_2 T) - \frac{1}{2}\right)\left(\left(-18 + \left(18 + (\omega+2)m^2 + 6m\right)\gamma_2^2\right)\right.\right.\right.\\
&(m-6)\beta_3^2\cosh^4(\gamma_2 T) - \left(-18 + \left(18 + (\omega+2)m^2 + 6m\right)\gamma_2^2\right)\\
&(m-6)\beta_3^2\cosh^2(\gamma_2 T) + \frac{1}{4}(m-18)\gamma_2^2\left(\frac{-27}{2} + \left(-54 + (\omega+2)m^2 - 6m\right)\beta_3^2\right)\Big)\\
&\left(\frac{\gamma_2}{\beta_3}\operatorname{cosech}(2\gamma_2 T)\right)^{(-m/6)} + 288\left(\gamma_2\cosh^2(\gamma_2 T)\sinh(\gamma_2 T)\zeta_1\right.\\
&\left.+\frac{3}{2}\cosh^3(\gamma_2 T)\zeta_0 - \frac{\gamma_2}{2}\sinh(\gamma_2 T)\zeta_1 - \frac{3}{2}\cosh(\gamma_2 T)\zeta_0\right)\pi\cosh(\gamma_2 T)\\
&\left.\left.\beta_3^3\left(\frac{\gamma_2}{\beta_3}\operatorname{cosech}(2\gamma_2 T)\right)^{(1/2)}\right)\right)\Big\},
\end{aligned} \tag{96}$$

$$\begin{aligned}
\Upsilon_{22} = &\left(\cosh(2\gamma_2 T)\left(\cosh^{(m/3)}(\theta)\left(\frac{\gamma_2}{\beta_3}\operatorname{cosech}(2\gamma_2 T)\right)^{(-m/6)}\sqrt{2}\left((m-6)\left(18 + \left(m^2\omega - 6m + 18\right)\gamma_2^2\right)\beta_3^2\right.\right.\right.\\
&\cosh^4(\gamma_2 T) - (m-6)\left(18 + \left(m^2\omega - 6m + 18\right)\gamma_2^2\right)\beta_3^2\cosh^2(\gamma_2 T) + \frac{1}{4}(m-18)\left(\frac{9}{2} + \left(m^2\omega - 6m + 18\right)\gamma_3^2\right)\gamma_2\Big)\\
&\left.\left.\left(\frac{\gamma_2}{\beta_3}\operatorname{cosech}(\gamma_2 T)\operatorname{sech}(\gamma_2 T)\right)^{(1/2)} - 864\pi\beta_3^2\beta_4\cosh^2(\gamma_2 T)\left(\cosh^2(\gamma_2 T) - 1\right)\right)\right)\Big\}.
\end{aligned}$$

For the BT-IX VHDE cosmological model, where

$$v_s^2 = \frac{\Upsilon_{23}}{\Upsilon_{24}}, \tag{97}$$

$$\Upsilon_{23}=\left(2\left(\frac{\gamma_3}{\beta_5}\operatorname{sech}(2\gamma_3T)\right)^{1/2}\left(\cosh(\gamma_3T)\sinh(\gamma_3T)\sin^{\frac{m}{3}}(\theta)\left(\left(-18+\left(18+(\omega+2)m^2+6m\right)\gamma_3^2\right)\beta_5^2(m-6)\cosh^4(\gamma_3T)-\left(-18+\left(18+(\omega+2)m^2+6m\right)\gamma_3^2\right)\beta_5^2(m-6)\cosh^2(\gamma_3T)+\left(\left(-270+(3\omega+9)m^2-18m\right)\gamma_3^2+27-\frac{9m}{2}\right)\beta_5^2-\frac{27\gamma_3^2}{8}(m-18)\right)\left(\frac{\gamma_3}{\beta_5}\operatorname{sech}(2\gamma_3T)\right)^{-m/6}\right.\right.$$
$$\left.\left.-288\left(\cosh^2(\gamma_3T)-\frac{1}{2}\right)\pi\left(\gamma_3\cosh(\gamma_3T)\sinh(\gamma_3T)\zeta_1+\frac{3\cosh^2(\gamma_3T)\zeta_0}{2}-\frac{3\zeta_0}{4}\right)\beta_5^2\right)\right\},$$

$$\Upsilon_{24}=\left\{\left(\sinh(2\gamma_3T)\left(\left(\frac{\gamma_3}{\beta_5}\cosh(2\gamma_3T)\right)^{-m/6}\sin^{m/3}(\theta)\left(\left(-18+\left(m^2\omega-6m+18\right)\gamma_3^2\right)\beta_5^2(m-6)\cosh^4(\gamma_3T)-\left(-18+\left(m^2\omega-6m+18\right)\gamma_3^2\right)\beta_5^2(m-6)\cosh^2(\gamma_3T)+\left(\left(3m^2\omega-18m+54\right)\gamma_3^2+27-\frac{9m}{2}\right)\beta_5^2+\frac{9\gamma_3^2}{8}(m-18)\right)\left(\frac{\gamma_3}{\beta_5\left(2\cosh^2(\gamma_3T)-1\right)}\right)^{1/2}\right.\right.\right.$$
$$\left.\left.\left.-432\left(\cosh^2(\gamma_3T)-\frac{1}{2}\right)^2\pi\beta_5^2\beta_6\right)\right)\right\}. \tag{98}$$

We have plotted the squared speed of the sound (v_s^2) versus redshift for three different values of ζ_0 and ζ_1 for BT-II, VIII, and IX models in Figures 22–24. The v_s^2 of BT-II and VIII models show the unstable behavior for three values of ζ_0 and ζ_1. Whereas, v_s^2 of BT-IX gives the stable to unstable behavior. Also, by increasing the values of ζ_0 and ζ_1, *i.e.*, increasing bulk viscosity, the models indicate the unstable behavior of the Universe.

4.7. Density Parameter (Ω_{vhde}). The dimensionless density parameter of DE (Ω_{vhde}) is defined as

$$\Omega_{vhde}=\frac{\rho_{vhde}}{3H^2}. \tag{99}$$

We were able to obtain the density parameter for our VHDE model by substituting the expressions for the Hubble parameter (H) and the energy density (ρ_{vhde}) in the above equation, and we used a graphical representation to analyze its behavior. The density parameter of BT-II, VIII, and IX models, respectively are given by

$$\Omega_{vhde}=\frac{\Upsilon_{25}}{6\gamma_1^2(2n+1)^2\pi}, \tag{100}$$

where

$$\Upsilon_{25}=\left(\left(-72\pi\beta_2(2\beta_1-2T\gamma_1)^{n+1/2}(T\gamma_1-\beta_1)+(2\beta_1-2T\gamma_1)^{m(-2n-1)+12n/6}\left(\gamma_1^2\omega\left(n+\frac{1}{2}\right)^2m^2-6\left(n+\frac{1}{2}\right)^2m\gamma_1^2+\frac{9}{8}\right.\right.\right.$$
$$\left.\left.\left.+\left(\frac{-9n^2}{2}-9n\right)\gamma_1^2\right)\right)(T\gamma_1-\beta_1)\right)\right\}, \tag{101}$$

$$\Omega_{vhde}=\frac{\Upsilon_{26}}{96\gamma_2^2\pi\beta_3^3\sinh(2\gamma_2T)\cosh^2(2\gamma_2T)}, \tag{102}$$

where

$$\Upsilon_{26}=\left(-2\gamma_2(\cosh(\theta))^{m/3}\left(\frac{\gamma_2}{\beta_3}\operatorname{cosech}(2\gamma_2T)\right)^{-m/6}\left(\left(18+\left(m^2\omega-6m+18\right)\gamma_2^2\right)\beta_3^2\cosh^2(2\gamma_2T)-18\beta_3^2+\frac{9\gamma_2^2}{2}\right)\right.$$
$$\left.-288\beta_4\left(\frac{\gamma_2}{\beta_3}\operatorname{cosech}(2\gamma_2T)\right)^{1/2}\sinh^3(2\gamma_2T)\pi\beta_3^3\right)\cosh^2(2\gamma_2T)-1\left.\right\}, \tag{103}$$

$$\Omega_{vhde}=\frac{\Upsilon_{27}}{96\gamma_3^2\cosh(2\gamma_3T)\pi\beta_5^3\sinh^2(2\gamma_3T)}, \tag{104}$$

where

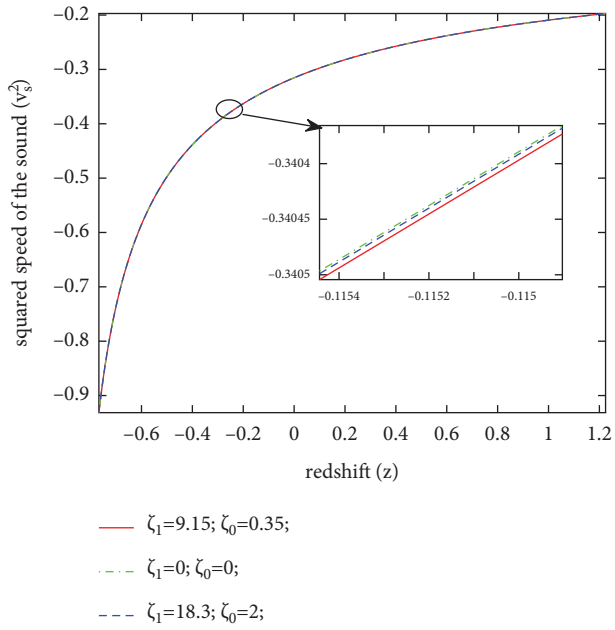

Figure 22: Squared speed of sound (v^2) versus redshift (z) for BT-II.

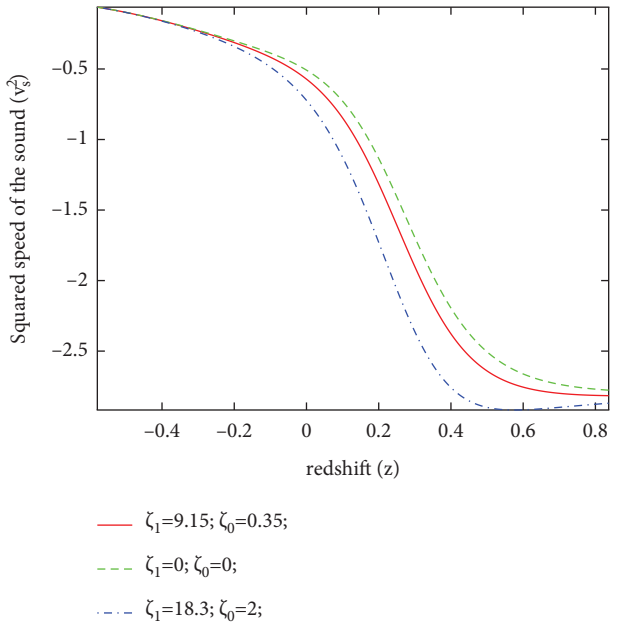

Figure 23: Squared speed of sound (v_s^2) versus redshift (z) for BT-VIII.

$$\Upsilon_{27} = \left(-2\left(\left(-18 + \left(m^2\omega - 6m + 18\right)\gamma_3^2\right)\beta_5^2 \cosh^2(2\gamma_3 T) - \gamma_3^2\left(\frac{-9}{2} + \left(m^2\omega - 6m + 18\right)\beta_5^2\right)\right)\gamma_3\left(\frac{\gamma_3}{\beta_5}\operatorname{sech}(2\gamma_3 T)\right)^{-m/6} \right.$$
$$\left. - 288\beta_6\left[\frac{\gamma_3}{\beta_5}\operatorname{sech}(2\gamma_3 T)\right]^{1/2}\pi\beta_5^3\cosh^3(2\gamma_3 T)\right)\Bigg\}. \tag{105}$$

The density parameter Ω_{vhde} for BT–II, VIII, and IX VHDE models against redshift (z) is seen in Figures 25–27,

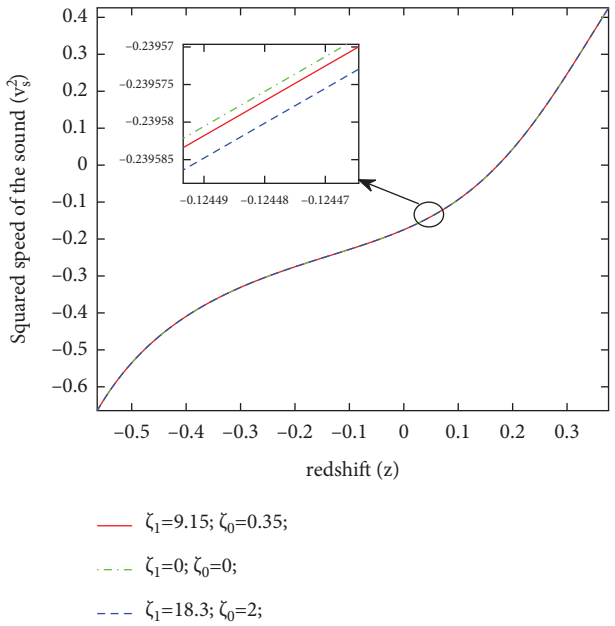

FIGURE 24: Squared speed of sound (v_s^2). versus redshift (z) for BT-IX.

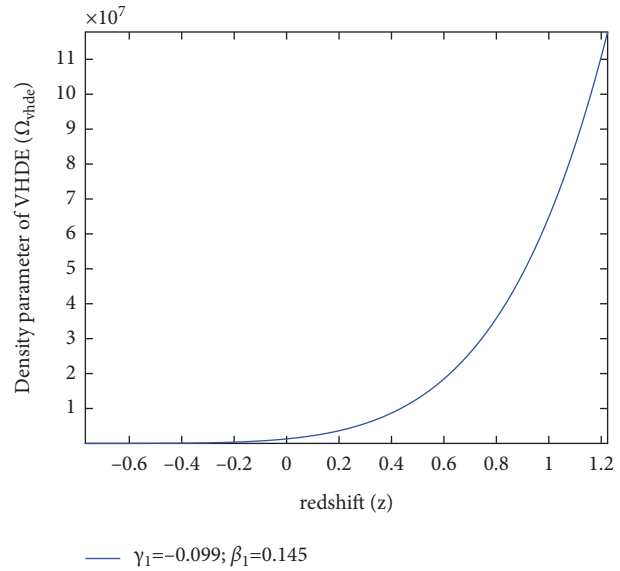

FIGURE 25: Density parameter of VHDE (Ω_{vhde}) versus redshift (z) for BT-II.

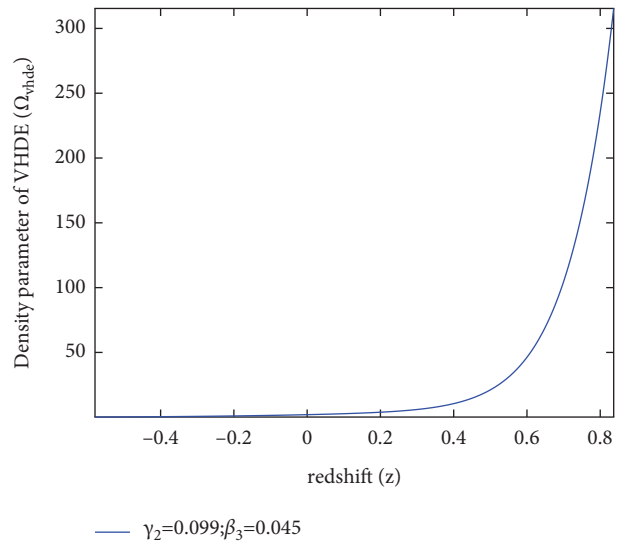

FIGURE 26: Density parameter of VHDE (Ω_{vhde}). versus redshift (z) for BT-VIII.

respectively. It can be seen that the trajectories of Ω_{vhde} are decreasing against redshift (z) for all the three models and are varying in the positive region.

4.8. Om-Diagnostic (Om(z)). To discriminate different phases of the Universe, Sahni et al., [130] have introduced another tool called the Om-diagnostic. It is also used to distinguish the ΛCDM for the nonminimally coupled scalar field, quintessence model, and phantom field through the trajectories of the curves. The phantom DE era corresponds to the positive trajectory, whereas the negative trajectory indicates that the DE constitutes quintessence. The om-diagnostic function is defined as

$$Om(z) = \frac{H^2(z) - H_0^2}{H_0^2\left(z^3 - 1\right)}. \tag{106}$$

The Om-diagnostic for models which are in Equations (35), (48), and (61) are, respectively, given by

$$\mathrm{Om}(z) = \frac{\gamma_1(2n+1) - 3H_0^2\left((1+z)/a_0\right)^{(6/2n+1)}}{3H_0^2\left((1+z)/a_0\right)^{(6/2n+1)}\left(z^3-1\right)},$$

$$\mathrm{Om}(z) = \frac{\left(\left(\gamma_2^2/9\right)\left(1+\left((\beta_3/\gamma_2)\cosh^2(\theta)\left((1+z)/a_0\right)^6\right)^2\right)\right) - H_0^2}{H_0^2\left(z^3-1\right)},$$

$$\mathrm{Om}(z) = \frac{\left(\left(\gamma_3^2/9\right)\left(1+\left((\beta_5/\gamma_3)\sin^2(\theta)\left((1+z)/a_0\right)^6\right)^2\right)\right) - H_0^2}{H_0^2\left(z^3-1\right)}. \tag{107}$$

The plots of the Om-diagnostic against redshift (z) are represented for the BT–II, VIII, and IX models in Figures 28–30, respectively, which depict the quintessence behavior of the DE, as the trajectories for the three models vary in the negative region.

5. Interpretations of the Models

To understand the cosmological mysteries of accelerated expansion, we have constructed the field equations of BDT for BT-II, VIII, and IX Universe in the context of VHDE. The exact solutions of the Brans–Dicke field equations are obtained by considering the relations between the metric potentials, the relation between scalar field and scale factor, and by taking bulk viscosity as proposed by Ren and Meng [105] and Meng et al., [106]. Furthermore, we have discussed the evolution of the Universe by studying various

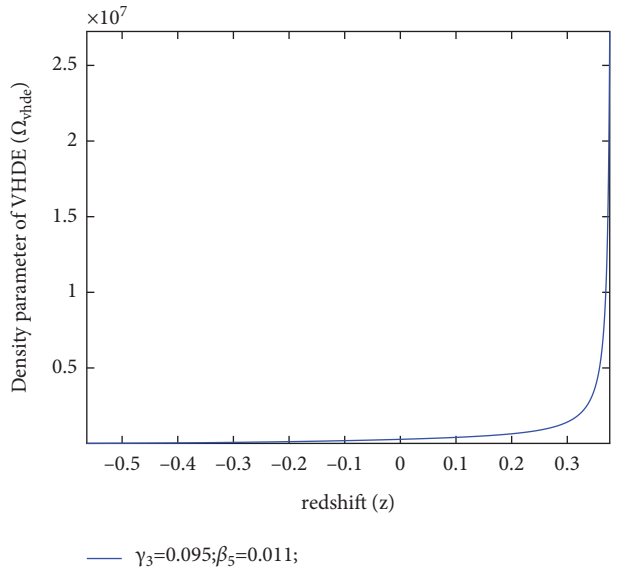

Figure 27: Density parameter of VHDE (Ω_{vhde}) versus redshift (z) for BT-IX.

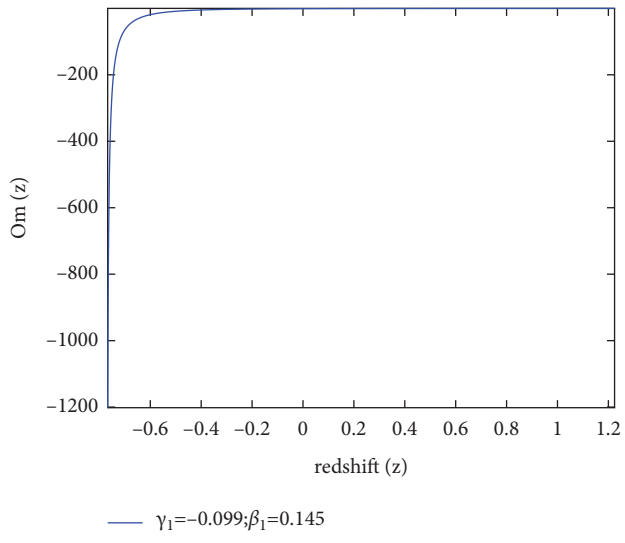

Figure 28: Om-diagnostics (Om(z)) versus. redshift (z) for BT-II.

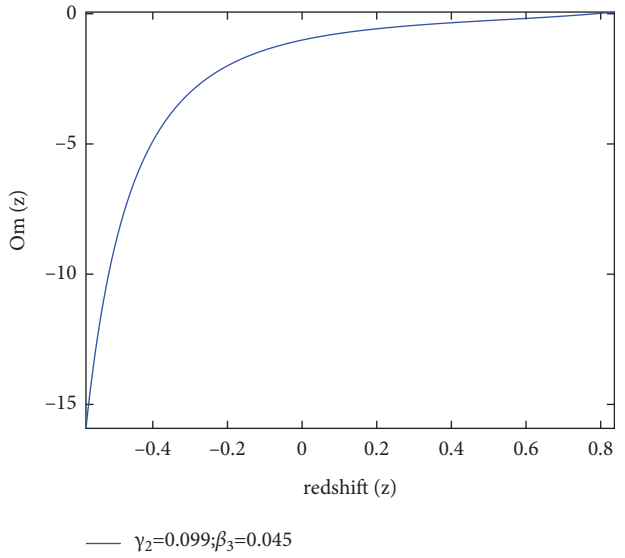

Figure 29: Om-diagnostics (Om(z)) versus redshift (z) for BT-VIII.

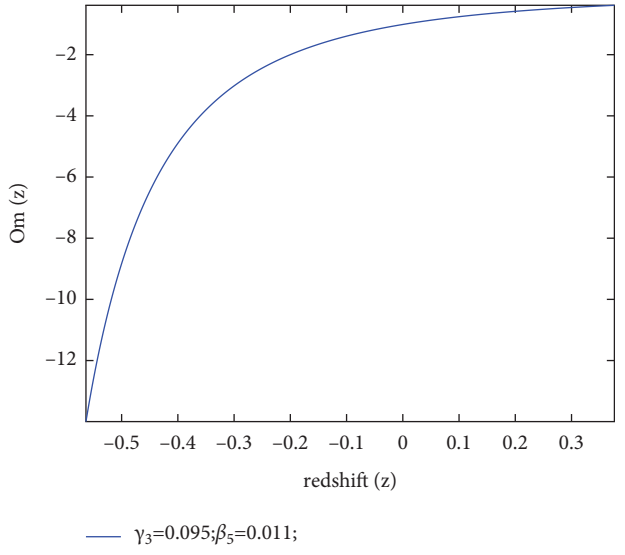

Figure 30: Om-diagnostics (Om(z)) versus. redshift (z) for BT-IX.

geometrical and physical parameters. We have plotted VHDE pressure, EoS parameter, EoS plane, and the squared speed of the sound by taking various values of ζ_0 & ζ_1. Also, a comparison study has been conducted by considering some isotropic and homogeneous cosmological models. Now, we summarize the results of the obtained models as follows:

For the Bianchi type-II cosmological model, we observe that the Universe shows a rapid expansion, as the VHDE pressure and energy density vary in negative and positive regions, respectively. This is further justified by the bulk viscosity coefficient (ζ) as, it is varying in the positive region throughout the cosmic evolution. We have constructed plots for various parameters and have observed that the deceleration parameter (q), the jerk parameter (j), and the statefinder plane ($r - s$) behave independently of time. The Universe shows a quintom-like nature, which is interpreted with the help of the EoS parameter; and the EoS plane varies in the freezing region. This behaviors of the EoS parameter and the EoS plane represents the accelerated expansion of the cosmos. The squared speed of sound (v_s^2) varies in the negative region, depicting an unstable Universe model. Also, the density parameter (Ω_{vhde}) is decreasing and varying in the positive region and the Om(z) differs in the negative region, depicting the quintessence behavior of the Universe.

The Bianchi type-VIII cosmological model has an accelerated cosmic expansion as the VHDE pressure and energy density vary in the negative and positive regions, respectively. Also, ζ is varying in the positive region, indicating an accelerated expansion of the Universe. The deceleration parameter (q) shows a transition from an early

decelerating phase to a late accelerating phase, and the jerk parameter differs in a positive region approaching to one as $z \longrightarrow 0$. Moreover, the statefinder pair (r, s) starts its evolution from the quintessence and phantom regions and reaches the Λ CDM model (for $r = 1, s = 0$). The model shows an unstable behavior, as v_s^2 is varying in the negative region. The plot of the EoS parameter states that the model varies in the phantom region and the EoS plane differs in the freezing region. The density parameter is decreasing and varying in the positive region and the Om(z) varies in the negative region depicting, the quintessence behavior of the Universe.

For the Bianchi type-IX cosmological model, the plots for VHDE pressure, energy density, and viscosity coefficients indicate an accelerated cosmic expansion as they vary in negative, positive, and positive regions respectively. The curve of deceleration parameter (q) varies in the accelerated phase, whereas the jerk parameter (j) vary in the negative region, approaching to one in the near future as $z \longrightarrow 0$. The squared speed of sound varies in positive to negative region, depicting the stable to an unstable behavior of the Universe. Also, the statefinder pair starts its evolution from the quintessence and phantom regions and reaches the Λ CDM model (for $r = 1, \ s = 0$). The Universe shows the quintom region and is distinguished in the freezing region as the EoS parameter and EoS plane are varying in the negative region, respectively. The density parameter (Ω_{vhde}) and Om(z) have the same behavior as the other two models.

Now, it will be interesting to compare our BT–II, VIII, and IX VHDE models in BDT along with the other dark energy models in the literature with regard to the energy density of the VHDE (ρ_{vhde}) EoS parameter $(\omega_{vhde})r - s$ plane, the deceleration parameter (q), the density parameter of the VHDE (Ω_{vhde}) Om diagnostic, and bulk viscosity (ζ). We have considered some isotropic and homogeneous models for comparison study. Singh and Srivastava [102] have studied a flat FRW Universe filled with DM and viscous new HDE and they present four possible solutions for the model depending on the choice of the viscous term. Also, they have discussed the evolution of the cosmological quantities such as scale factor, deceleration parameter, and transition redshift to observe the effect of viscosity in the evolution. Srivastava and Singh [131] have investigated the new HDE model in modified $f(R, T)$ gravity theory within the framework of a flat FRW model with bulk viscous matter content and found the solution for nonviscous and viscous new HDE models. Also, they have analyzed a new HDE model with constant bulk viscosity (*i.e.*,$\zeta_1 = \zeta_0 =$ constant) to explain the present accelerated the expansion of the Universe. Singh and Kumar [132] have examined Ricci dark energy model with bulk viscosity to observe the cosmic accelerating expansion phenomena, and they analyzed the model with deceleration parameter (q), EoS parameter (ω_{vhde}), bulk viscosity (ζ), and Om(z). Singh and Kaur [133] have explored a matter-dominated model with a bulk viscosity in BDT to interpret the observed cosmic accelerating expansion phenomena with flat FRW line element. Kumar and Beesham [134] have studied the concept of HDE in the frame work of BDT in the formalism of the flat FRW metric, and they have shown that the VHDE can play the role of an interacting HDE as it is able to explain the phase transition of the Universe. Rahman and Ansari [135] have studied the interacting generalized ghost polytropic gas model of DE with a specific Hubble parameter in the spatially homogeneous and anisotropic LRS BT-II Universe in GR and also discuss the physical and geometrical properties of the Universe, which are found to be consistent with recent observations. Maurya et al., [136] have studied DE models in LRS BT-II space-time in a new perspective of time-dependent deceleration parameters in GR where various parameters of DE models are also calculated, and it is found that these are consistent with the recent observations. Naidu [137] has investigated the spatially homogeneous and totally anisotropic BT-II cosmological model filled with pressure less matter and anisotropic modified Ricci dark energy in the presence of an attractive massive scalar field in GR. It seems that the deceleration parameter(q) of our BT-VIII model coincides with the results of Singh and Srivastava [102], Singh and Kumar [132], Singh and Kaur [133], Kumar and Beesham [134], Rahman and Ansari [135], and Maurya et al. [136]. Also, the deceleration parameter(q) of our BT-IX model coincides with the results of Kumar and Beesham [134] and Maurya et al., [136]. The state finder parameters $(r - s)$ of the BT-VIII & IX models coincide with the results of Singh and Srivastava [102], Srivastava and Singh [131], Singh and Kumar [132], Singh and Kaur [133], Kumar and Beesham [134], Rahman and Ansari [135], and Naidu [137]. The EoS parameters of our BT-II, VIII, and IX VHDE models coincide with the results of Maurya et al., [136] and Naidu [137]. Whereas, at null viscosity, the EoS parameter of our BT-VIII model agrees with the results of Singh and Kumar [132], Singh and Kaur [133], and Rahman and Ansari [135]. The density parameter of our BT-II, VIII, and IX VHDE models agrees with the results of Rahman and Ansari [135] and Naidu [137]. The Om-diagnostics of our BT-II, VIII, and IX VHDE models correspond with the results of Singh and Srivastava [102], Srivastava and Singh [131], Singh and Kumar [132], and Singh and Kaur [133]. The energy density of the VHDE of our BT-II, VIII, and IX models agree with the results of Rahman and Ansari [135] and Maurya et al., [136]. The bulk viscosity of our models coincides with the results of Singh and Kumar [132]. The above results lead to the conclusion that our BT-II, VIII, and IX VHDE models in BDT are in good agreement with the observational data. Also, we hope that the above investigations will help to have a deep insight into the behavior of bulk viscosity with VHDE Universes.

Data Availability

The data used to support the findings of this study are included within the article.

Conflicts of Interest

The authors declare that they have no conflicts of interest.

Authors' Contributions

The study was carried out in collaboration of all authors. All authors read and approved the final manuscript.

Acknowledgments

MVS acknowledges the Department of Science and Technology (DST), Govt of India, New Delhi for financial support to carry out the Research Project (No. EEQ/2021/000737, Dt. 07/03/2022).

References

[1] A. Einstein, *Relativity: "The Special and General Theory"*, H. Holt and Company, NY, 1920.

[2] D. Bohm, *The Special Theory of Relativity*, Routledge, Oxfordshire, England, UK, 2015.

[3] S. Hawking and R. Penrose, *The Nature of Space and Time*, Vol. 3, Princeton University Press, Princeton, NJ, USA, 2010.

[4] A. Einstein and M. Grossmann, "Outline of a generalized theory of relativity and of a theory of gravitation. I. Physical part by A. Einstein II," *Mathematical part by M. Grossmann. Z. Math. Phys*, vol. 62, pp. 225–245, 1913.

[5] E. Mach, *The Science of Mechanics: A Critical and Historical Account of its Development. Supplement*, Open court publishing Company, Chicago, 1915.

[6] W. T. Ni, "Empirical foundations of the relativistic gravity," *International Journal of Modern Physics D*, vol. 14, no. 06, pp. 901–921, 2005.

[7] C. M. Will, "The confrontation between general relativity and experiment," *Living Reviews in Relativity*, vol. 17, no. 1, pp. 4–117, 2014.

[8] S. G. Turyshev, "Experimental tests of general relativity: recent progress and future directions," *Physics-Uspekhi*, vol. 52, no. 1, pp. 1–27, 2009.

[9] A. Ashtekar, *100 Years Of Relativity: Space-Time Structure-Einstein and beyond*, World Scientific, Singapore, 2005.

[10] T. Padmanabhan, "One hundred years of General Relativity: summary, status and prospects," *Current Science*, vol. 109, no. 7, pp. 1215–1219, 2015.

[11] C. H. Brans and R. H. Dicke, "Mach's principle and a relativistic theory of gravitation. II," *Physical Review*, vol. 125, no. 6, pp. 2194–2201, 1962.

[12] S. Das and N. Banerjee, "Brans-Dicke scalar field as a chameleon," *Physical Review D*, vol. 78, no. 4, Article ID 043512, 2008.

[13] B. Bertotti, L. Iess, and P. Tortora, "A test of general relativity using radio links with the Cassini spacecraft," *Nature*, vol. 425, no. 6956, pp. 374–376, 2003.

[14] S. Rama and S. Ghosh, "Short-distance repulsive gravity as a consequence of the non-trivial PPN parameters β and γ," *Physics Letters B*, vol. 383, no. 1, pp. 31–38, 1996.

[15] S. Kalyana Rama, "Some cosmological consequences of non-trivial PPN parameters β and γ," *Physics Letters B*, vol. 373, no. 4, pp. 282–288, 1996.

[16] A. Linde, "Extended chaotic inflation and spatial variations of the gravitational constant," *Physics Letters B*, vol. 238, no. 2-4, pp. 160–165, 1990.

[17] O. Bertolami and P. J. Martins, "Nonminimal coupling and quintessence," *Physical Review D*, vol. 61, no. 6, Article ID 064007, 2000.

[18] H. Kim, "Brans-Dicke theory as a unified model for dark matter-dark energy," *Monthly Notices of the Royal Astronomical Society*, vol. 364, no. 3, pp. 813–822, 2005.

[19] T. Clifton and J. D. Barrow, "Decaying gravity," *Physical Review D*, vol. 73, no. 10, Article ID 104022, 2006.

[20] B. K. Sahoo and L. P. Singh, "Time dependence of brans–dicke parameter ω for an expanding universe," *Modern Physics Letters A*, vol. 17, no. 36, pp. 2409–2415, 2002.

[21] P. G. Bergmann, "Comments on the scalar-tensor theory," *International Journal of Theoretical Physics*, vol. 1, no. 1, pp. 25–36, 1968.

[22] R. V. Wagoner, "Scalar-tensor theory and gravitational waves," *Physical Review D*, vol. 1, no. 12, pp. 3209–3216, 1970.

[23] K. Nordtvedt Jr, "Post-Newtonian metric for a general class of scalar-tensor gravitational theories and observational consequences," *The Astrophysical Journal*, vol. 161, no. 1059, 1970.

[24] N. Banerjee and D. Pavon, "Cosmic acceleration without quintessence," *Physical Review D*, vol. 63, no. 4, Article ID 043504, 2001.

[25] N. Banerjee and K. Ganguly, "Generalized scalar-tensor theory and the cosmic acceleration," *International Journal of Modern Physics D*, vol. 18, no. 03, pp. 445–451, 2009.

[26] W. Chakraborty and U. Debnath, "Role of Brans-Dicke Theory with or without self-interacting potential in cosmic acceleration," *International Journal of Theoretical Physics*, vol. 48, no. 1, pp. 232–247, 2009.

[27] M. Jamil and D. Momeni, "Evolution of the brans-dicke parameter in generalized chameleon cosmology," *Chinese Physics Letters*, vol. 28, no. 9, Article ID 099801, 2011.

[28] J. Satish and R. Venkateswarlu, "Behaviour of Brans-Dicke parameter in generalised chameleon cosmology with Kantowski-Sachs space-time," *Eur.Phys.J.Plus*, vol. 129, no. 12, pp. 275–278, 2014.

[29] S. Roy, "Time evolution of the matter content of the expanding universe in the framework of Brans-Dicke gravity," *Research in Astronomy and Astrophysics*, vol. 19, no. 4, Article ID 061, 2019.

[30] S. Roy, S. Chattopadhyay, and A. Pasqua, "A study on the dependence of the dimensionless Brans-Dicke parameter on the scalar field and their time dependence," *Eur.Phys.J.Plus*, vol. 128, no. 12, pp. 147–216, 2013.

[31] A. Chand, R. K. Mishra, and A. Pradhan, "FRW cosmological models in Brans-Dicke theory of gravity with variable q q and dynamical Λ $\varLambda$ -term," *Astrophysics and Space Science*, vol. 361, no. 2, pp. 81–12, 2016.

[32] S. Das and A. Al Mamon, "An interacting model of dark energy in Brans-Dicke theory," *Astrophysics and Space Science*, vol. 351, no. 2, pp. 651–660, 2014.

[33] A. H. Taub, "Empty space-times admitting a three parameter group of motions," *Annals of Mathematics*, vol. 53, no. 3, pp. 472–490, 1951.

[34] C. W. Misner, "Mixmaster universe," *Physical Review Letters*, vol. 22, no. 20, pp. 1071–1074, 1969.

[35] N. J. Cornish and J. J. Levin, "The mixmaster universe is chaotic," *Physical Review Letters*, vol. 78, no. 6, pp. 998–1001, 1997.

[36] X. F. Lin and R. M. Wald, "Proof of the closed-universe-recollapse conjecture for diagonal Bianchi type-IX cosmologies," *Physical Review D*, vol. 40, no. 10, pp. 3280–3286, 1989.

[37] X. F. Lin and R. M. Wald, "Proof of the closed-universe recollapse conjecture for general Bianchi type-IX cosmologies," *Physical Review D*, vol. 41, no. 8, pp. 2444–2448, 1990.

[38] V. U. M. Rao and M. Vijaya Santhi, "Bianchi type-II, VIII & IX perfect fluid magnetized cosmological models in Brans-Dicke theory of gravitation," *Astrophysics and Space Science*, vol. 337, no. 1, pp. 387–392, 2012.

[39] M. Vijaya Santhi, T. CH. Naidu, and D. CH. Papa Rao, *Some Bianchi Type Bulk Viscous String Cosmological Models in F (R) Gravity*, IOP Publishing, vol. 1344, p. 012036, Bristol, UK, 2019.

[40] K. V. Sireesha and V. U. M Rao, "Bianchi type-II, VIII & IX holographic dark energy cosmological models in brans-dicke theory of gravitation," *The Afri.Rev.Phys.* vol. 14, 2019.

[41] V. U. M. Rao and K. V. S. Sireesha, "Bianchi type-II, VIII & IX cosmological models with strange quark matter attached to string cloud in Brans–Dicke and general theory of gravitation," *International Journal of Theoretical Physics*, vol. 52, no. 4, pp. 1240–1249, 2013.

[42] S. Perlmutter, G. Aldering, G. Goldhaber et al., "Measurements of Ω and Λ from 42 high- redshift supernovae," *The Astrophysical Journal*, vol. 517, no. 2, pp. 565–586, Jun 1999.

[43] A. G. Riess, A. V. Filippenko, P. Challis et al., "Observational evidence from supernovae for an accelerating universe and a cosmological constant," *The Astronomical Journal*, vol. 116, no. 3, pp. 1009–1038, 1998.

[44] R. R. Caldwell and M. Doran, "Cosmic microwave background and supernova constraints on quintessence: concordance regions and target models," *Physical Review D*, vol. 69, no. 10, Article ID 103517, 2004.

[45] Z. Yi. Huang, B. Wang, E. Abdalla, and R. K. Su, "Holographic explanation of wide- angle power correlation suppression in the cosmic microwave background radiation," *Journal of Cosmology and Astroparticle Physics*, vol. 2006, no. 05, p. 013, 2006.

[46] S. F. Daniel, R. R. Caldwell, A. Cooray, and A. Melchiorri, "Large scale structure as a probe of gravitational slip," *Physical Review D*, vol. 77, no. 10, Article ID 103513, 2008.

[47] B. Ratra and P. J. E. Peebles, "Cosmological consequences of a rolling homogeneous scalar field," *Physical Review D*, vol. 37, no. 12, pp. 3406–3427, 1988.

[48] Ch. Wetterich, "Cosmology and the fate of dilatation symmetry," *Nuclear Physics B*, vol. 302, no. 4, pp. 668–696, 1988.

[49] R. R. Caldwell, R. Dave, and P. J. Steinhardt, "Cosmological imprint of an energy component with general equation of state," *Physical Review Letters*, vol. 80, no. 8, pp. 1582–1585, 1998.

[50] I. Zlatev, L. Wang, and P. J. Steinhardt, "Quintessence, cosmic coincidence, and the cosmological constant," *Physical Review Letters*, vol. 82, no. 5, pp. 896–899, 1999.

[51] R. R. Caldwell, "A phantom menace? Cosmological consequences of a dark energy component with super-negative equation of state," *Physics Letters B*, vol. 545, no. 1-2, pp. 23–29, 2002.

[52] S.'ichi Nojiri and S. D. Odintsov, "Quantum de Sitter cosmology and phantom matter," *Physics Letters B*, vol. 562, no. 3-4, pp. 147–152, 2003.

[53] Y. H. Wei and Y. U. Tian, "SO (1, 1) dark energy model and the universe transition," *Classical and Quantum Gravity*, vol. 21, no. 23, pp. 5347–5353, 2004.

[54] M. R. Setare, "Interacting holographic phantom," *European Physical Journal C: Particles and Fields*, vol. 50, no. 4, pp. 991–998, 2007.

[55] B. O. Feng, X. Wang, and X. Zhang, "Dark energy constraints from the cosmic age and supernova," *Physics Letters B*, vol. 607, no. 1-2, pp. 35–41, 2005.

[56] Y. F. Cai, E. N. Saridakis, M. R. Setare, and J. Q. Xia, "Quintom cosmology: theoretical implications and observations," *Physics Reports*, vol. 493, no. 1, pp. 1–60, 2010.

[57] A. Sen, "Tachyon matter," *Journal of High Energy Physics*, vol. 2002, no. 07, p. 065, 2002.

[58] T. Padmanabhan, "Accelerated expansion of the universe driven by tachyonic matter," *Physical Review D*, vol. 66, no. 2, Article ID 021301, 2002.

[59] M. R. Setare, J. Sadeghi, and A. R. Amani, "Interacting tachyon dark energy in non-flat universe," *Physics Letters B*, vol. 673, no. 4-5, pp. 241–246, 2009.

[60] Ch. Armendariz-Picon, V. Mukhanov, and P. J. Steinhardt, "Dynamical solution to the problem of a small cosmological constant and late-time cosmic acceleration," *Physical Review Letters*, vol. 85, no. 21, pp. 4438–4441, 2000.

[61] A. Kamenshchik, U. Moschella, and V. Pasquier, "An alternative to quintessence," *Physics Letters B*, vol. 511, no. 2-4, pp. 265–268, 2001.

[62] M. C. Bento, O. Bertolami, and A. A. Sen, "Generalized Chaplygin gas, accelerated expansion, and dark-energy-matter unification," *Physical Review D*, vol. 66, no. 4, Article ID 043507, 2002.

[63] U. Debnath, A. Banerjee, and S. Chakraborty, "Role of modified Chaplygin gas in accelerated universe," *Classical and Quantum Gravity*, vol. 21, no. 23, pp. 5609–5617, 2004.

[64] Z. H. Zhu, "Generalized Chaplygin gas as a unified scenario of dark matter/energy: observational constraints," *Astronomy & Astrophysics*, vol. 423, no. 2, pp. 421–426, 2004.

[65] M. R. Setare, "Holographic Chaplygin gas model," *Physics Letters B*, vol. 648, no. 5-6, pp. 329–332, 2007.

[66] L. Xu, J. Lu, and Y. Wang, "Revisiting generalized Chaplygin gas as a unified dark matter and dark energy model," *European Physical Journal C: Particles and Fields*, vol. 72, no. 2, pp. 1883–1886, 2012.

[67] Y. Wang, D. Wands, L. Xu, J. De-Santiago, and A. Hojjati, ""Cosmological constraints on a decomposed" Chaplygin gas," *Physical Review D*, vol. 87, no. 8, Article ID 083503, 2013.

[68] H. Saadat and B. Pourhassan, "FRW bulk viscous cosmology with modified cosmic Chaplygin gas," *Astrophysics and Space Science*, vol. 344, no. 1, pp. 237–241, 2013.

[69] B. Pourhassan and E. O. Kahya, "FRW cosmology with the extended Chaplygin gas," *Advances in High Energy Physics*, vol. 2014, Article ID 231452, pp. 1–11, 2014.

[70] E. O. Kahya and B. Pourhassan, "Observational constraints on the extended Chaplygin gas inflation," *Astrophysics and Space Science*, vol. 353, no. 2, pp. 677–682, 2014.

[71] E. O. Kahya and B. Pourhassan, "The universe dominated by the extended Chaplygin gas," *Modern Physics Letters A*, vol. 30, no. 13, Article ID 1550070, 2015.

[72] E. O. Kahya, M. Khurshudyan, B. Pourhassan, R. Myrzakulov, and A. Pasqua, "Higher order corrections of the extended Chaplygin gas cosmology with varying G and Λ," *European Physical Journal C: Particles and Fields*, vol. 75, no. 2, pp. 1–12, 2015.

[73] J. Sadeghi, H. Farahani, and B. Pourhassan, "Interacting holographic extended Chaplygin gas and phantom cosmology in the light of BICEP2," *Eur.Phys.J.Plus*, vol. 130, no. 4, pp. 84–89, 2015.

[74] B. Pourhassan, "Unified universe history through phantom extended Chaplygin gas," *Canadian Journal of Physics*, vol. 94, no. 7, pp. 659–670, 2016.

[75] J. Sadeghi, M. Khurshudyan, and H. Farahani, "Phenomenological varying modified chaplygin gas with variable G and Λ: toy models for our universe," *International Journal of Theoretical Physics*, vol. 55, no. 1, pp. 81–97, 2016.

[76] M. Li, "A model of holographic dark energy," *Physics Letters B*, vol. 603, no. 1-2, pp. 1–5, 2004.

[77] L. Susskind, "The world as a hologram," *Journal of Mathematical Physics*, vol. 36, no. 11, pp. 6377–6396, 1995.

[78] P. Hořava and D. Minic, "Probable values of the cosmological constant in a holographic theory," *Physical Review Letters*, vol. 85, no. 8, pp. 1610–1613, 2000.

[79] S. Thomas, "Holography stabilizes the vacuum energy," *Physical Review Letters*, vol. 89, no. 8, Article ID 081301, 2002.

[80] S. D. H. Hsu, "Entropy bounds and dark energy," *Physics Letters B*, vol. 594, no. 1-2, pp. 13–16, 2004.

[81] S. Wang, Y. Wang, and M. Li, "Holographic dark energy," *Physics Reports*, vol. 696, pp. 1–57, 2017.

[82] A. G. Cohen, D. B. Kaplan, and A. E. Nelson, "Effective field theory, black holes, and the cosmological constant," *Physical Review Letters*, vol. 82, no. 25, pp. 4971–4974, 1999.

[83] B. Guberina, R. Horvat, and H. Nikolic´, "Non-saturated holographic dark energy," *Journal of Cosmology and Astroparticle Physics*, vol. 2007, no. 01, Article ID 012, 2007.

[84] J. D. Bekenstein, "Black holes and entropy," *Physical Review D*, vol. 7, no. 8, pp. 2333–2346, 1973.

[85] S. W. Hawking, "Particle creation by black holes," *Communications in Mathematical Physics*, vol. 43, no. 3, pp. 199–220, 1975.

[86] G. Hooft, "Dimensional reduction in quantum gravity," 1993, https://arxiv.org/abs/gr-qc/9310026.

[87] J. Maldacena, "The large-N limit of superconformal field theories and supergravity," *International Journal of Theoretical Physics*, vol. 38, no. 4, pp. 1113–1133, 1999.

[88] A. Strominger, "The dS/CFT correspondence," *Journal of High Energy Physics*, vol. 2001, no. 10, Article ID 034, 2001.

[89] H. Liu, K. Rajagopal, and U. A. Wiedemann, "Wilson loops in heavy ion collisions and their calculation in AdS/CFT," *Journal of High Energy Physics*, vol. 2007, no. 03, p. 066, 2007.

[90] S. Nojiri and S. D. Odintsov, "Unifying phantom inflation with late-time acceleration: scalar phantom–non-phantom transition model and generalized holographic dark energy," *General Relativity and Gravitation*, vol. 38, no. 8, pp. 1285–1304, 2006.

[91] S. Nojiri and S. D. Odintsov, "Covariant generalized holographic dark energy and accelerating universe," *European Physical Journal C: Particles and Fields*, vol. 77, no. 8, pp. 528–8, 2017.

[92] N. Banerjee and D. Pavon, "Holographic dark energy in Brans–Dicke theory," *Physics Letters B*, vol. 647, no. 5-6, pp. 477–481, 2007.

[93] L. Xiang-Lai and Z. Xin, "New agegraphic dark energy in Brans–Dicke theory," *Communications in Theoretical Physics*, vol. 52, no. 4, pp. 761–768, 2009.

[94] A. Sheykhi, "Interacting holographic dark energy in Brans–Dicke theory," *Physics Letters B*, vol. 681, no. 3, pp. 205–209, 2009.

[95] A. Sheykhi, "Interacting new agegraphic dark energy in nonflat Brans-Dicke cosmology," *Physical Review D*, vol. 81, no. 2, Article ID 023525, 2010.

[96] P. Kumar and C. P. Singh, "New agegraphic dark energy model in Brans-Dicke theory with logarithmic form of scalar field," *Astrophysics and Space Science*, vol. 362, no. 3, pp. 52–58, 2017.

[97] C. P. Singh and P. Kumar, "Holographic dark energy in Brans-Dicke theory with logarithmic form of scalar field," *International Journal of Theoretical Physics*, vol. 56, no. 10, pp. 3297–3310, 2017.

[98] F. Felegary, F. Darabi, and M. R. Setare, "Interacting holographic dark energy model in Brans– Dicke cosmology and coincidence problem," *International Journal of Modern Physics D*, vol. 27, no. 03, Article ID 1850017, 2018.

[99] M. Srivastava and C. P. Singh, "Cosmological evolution of non-interacting and interacting holographic dark energy model in Brans–Dicke theory," *International Journal of Geometric Methods in Modern Physics*, vol. 15, no. 07, Article ID 1850124, 2018.

[100] L. Xu, W. Li, and J. Lu, "Holographic dark energy in Brans–Dicke theory," *European Physical Journal C: Particles and Fields*, vol. 60, no. 1, pp. 135–140, 2009.

[101] C. Eckart, "The thermodynamics of irreversible processes. III. Relativistic theory of the simple fluid," *Physical Review*, vol. 58, no. 10, pp. 919–924, 1940.

[102] C. P. Singh and M. Srivastava, "Viscous cosmology in new holographic dark energy model and the cosmic acceleration," *European Physical Journal C: Particles and Fields*, vol. 78, no. 3, pp. 190–216, 2018.

[103] C. B. Collins, E. N. Glass, and D. A. Wilkinson, "Exact spatially homogeneous cosmologies," *General Relativity and Gravitation*, vol. 12, no. 10, pp. 805–823, 1980.

[104] S. K. Tripathy, D. Behera, and B. Mishra, "Unified dark fluid in Brans–Dicke theory," *European Physical Journal C: Particles and Fields*, vol. 75, no. 4, pp. 149–211, 2015.

[105] J. Ren and X. H. Meng, "Cosmological model with viscosity media (dark fluid) described by an effective equation of state," *Physics Letters B*, vol. 633, no. 1, pp. 1–8, 2006.

[106] M. Xin-He, R. Jie, and H. Ming-Guang, "Friedmann cosmology with a generalized equation of state and bulk viscosity," *Communications in Theoretical Physics*, vol. 47, no. 2, pp. 379–384, 2007.

[107] M. S. Berman, "A special law of variation for Hubble's parameter," *Il Nuovo Cimento B Series 11*, vol. 74, no. 2, pp. 182–186, 1983.

[108] B. K. Bishi, S. K. J. Pacif, P. K. Sahoo, and G. P. Singh, "LRS Bianchi type-I cosmological model with constant deceleration parameter in f (R, T) gravity," *International Journal of Geometric Methods in Modern Physics*, vol. 14, no. 11, Article ID 1750158, 2017.

[109] M. V. Santhi, V. Rao, and Y. Aditya, "Bulk viscous string cosmological models in f (R) gravity," *Canadian Journal of Physics*, vol. 96, no. 1, pp. 55–61, 2018.

[110] M. Vijaya Santhi and T. Chinnappalanaidu, "Re´nyi holographic dark energy model in a scalar–tensor theory," *New Astronomy*, vol. 92, Article ID 101725, 2022.

[111] G. C. Samanta, "Universe filled with dark energy (DE) from a wet dark fluid (WDF) in f (R, T) gravity," *International Journal of Theoretical Physics*, vol. 52, no. 7, pp. 2303–2315, 2013.

[112] S. Kumar and C. P. Singh, "Anisotropic dark energy models with constant deceleration parameter," *General Relativity and Gravitation*, vol. 43, no. 5, pp. 1427–1442, 2011.

[113] M. Visser, "Cosmography: cosmology without the Einstein equations," *General Relativity and Gravitation*, vol. 37, no. 9, pp. 1541–1548, 2005.

[114] D. Rapetti, S. W. Allen, M. A. Amin, and R. D. Blandford, "A kinematical approach to dark energy studies," *Monthly Notices of the Royal Astronomical Society*, vol. 375, no. 4, pp. 1510–1520, 2007.

[115] M. Vijaya Santhi and T. Chinnappalanaidu, "Strange quark matter cosmological models attached to string cloud in f (R) theory of gravity," *Indian Journal of Physics*, vol. 96, no. 3, pp. 953–962, 2022.

[116] V. U. M. Rao, T. Vinutha, D. Neelima, and G. SuryaNarayana, "Bianchi type III, V & VI 0 universe in f (R, T) gravity," *The Afri.Rev.Phys.* vol. 10, 2015.

[117] M. Vijaya Santhi, V. U. M Rao, and Y. Aditya, "Holographic dark energy model with generalized chaplygin gas in a scalar-tensor theory of gravitation," *Prespacetime Journal*, vol. 7, no. 15, 2016.

[118] V. U. M Rao and U. Y. Divya Prasanthi, "Kantowski-sachs holographic dark energy in Brans- dicke theory of gravitation," *The Afri.Rev.Phys.* vol. 11, 2016.

[119] A. Y. Shaikh, S. V. Gore, and S. D. Katore, "Cosmic acceleration and stability of cosmological models in extended teleparallel gravity," *Pramana*, vol. 95, no. 1, pp. 16–10, 2021.

[120] G. Dvali, G. Gabadadze, and M. Porrati, "4D gravity on a brane in 5D Minkowski space," *Physics Letters B*, vol. 485, no. 1-3, pp. 208–214, 2000.

[121] V. Sahni, T. D. Saini, A. A. Starobinsky, and U. Alam, "Statefinder—a new geometrical diagnostic of dark energy," *Journal of Experimental and Theoretical Physics Letters*, vol. 77, no. 5, pp. 201–206, 2003.

[122] M. Vijaya Santhi, V. U. M. Rao, and Y. Aditya, "Kaluza-klein cosmological models with two fluids source in brans-dicke theory of gravitation," *The Afri.Rev.Phys.* vol. 11, 2016.

[123] G. C. Samanta and B. Mishra, "Anisotropic cosmological model in presence of holographic dark energy and quintessence," *Iran J.Sci.Technol Trans Sci.*vol. 41, no. 2, pp. 535–541, 2017.

[124] S. D. Katore and S. V. Gore, "ACDM cosmological models with quintessence in f (R) theory of gravitation," *Journal of Astrophysics & Astronomy*, vol. 41, no. 1, pp. 12–15, 2020.

[125] N. Aghanim, Y. Akrami, M. Ashdown et al., "Planck 2018 results-VI. Cosmological parameters," *Astronomy & Astrophys.* vol. 641, 2020.

[126] R. R. Caldwell and E. V. Linder, "Limits of quintessence," *Physical Review Letters*, vol. 95, no. 14, Article ID 141301, 2005.

[127] P. A. R. Ade, N. Aghanim, C. Armitage-Caplan et al., "Planck 2013 results. XVI. Cosmological parameters," *Astronomy & Astrophys.*vol. 571, no. A16, 2014.

[128] G. F. Hinshaw, "Nine-year Wilkinson microwave anisotropy probe (WMAP) observations: cosmology results," *The Astrophysical Journal*, vol. 208, no. 19H, 2013.

[129] Y. S. Myung, "Instability of holographic dark energy models," *Physics Letters B*, vol. 652, no. 5-6, pp. 223–227, 2007.

[130] V. Sahni, A. Shafieloo, and A. A. Starobinsky, "Two new diagnostics of dark energy," *Physical Review D*, vol. 78, no. 10, Article ID 103502, 2008.

[131] M. Srivastava and C. P. Singh, "New holographic dark energy model with constant bulk viscosity in modified f (R , T) $f(R, T)$ gravity theory," *Astrophysics and Space Science*, vol. 363, no. 6, pp. 117–215, 2018.

[132] C. P. Singh and A. Kumar, "Observational constraints on viscous Ricci dark energy model," *Astrophysics and Space Science*, vol. 364, no. 6, pp. 94–99, 2019.

[133] C. P. Singh and S. Kaur, "Probing bulk viscous matter-dominated model in Brans-Dicke theory," *Astrophysics and Space Science*, vol. 365, no. 1, pp. 2–12, 2020.

[134] P. Kumar, P. Kumar, and A. Beesham, "Reconsidering holographic dark energy in Brans– Dicke theory," *European Physical Journal C: Particles and Fields*, vol. 82, no. 2, pp. 143–210, 2022.

[135] M. A. Rahman and M. Ansari, "Interacting generalized ghost polytropic gas model of dark energy with a specific Hubble parameter in LRS Bianchi type-II universe," *Astrophysics and Space Science*, vol. 354, no. 2, pp. 675–682, 2014.

[136] D. C. Maurya, R. Zia, and A. Pradhan, "Dark energy models in LRS Bianchi type-II space-time in the new perspective of time-dependent deceleration parameter," *International Journal of Geometric Methods in Modern Physics*, vol. 14, no. 05, Article ID 1750077, 2017.

[137] R. L. Naidu, "Bianchi type-II modified holographic Ricci dark energy cosmological model in the presence of massive scalar field," *Canadian Journal of Physics*, vol. 97, no. 3, pp. 330–336, 2019.